COUPLED SOLUTE FLUXES IN MEMBRANE SYSTEMS

by

William R. Galey, Jr., B. S.

A THESIS
Presented to the Department of Biochemistry
and the Graduate Division of the University of Oregon Medical School
in partial fulfillment of
the requirements for the degree of
Doctor of Philosophy

June 1969

APPROVED:

[redacted]

....

(Professor in Charge of Thesis)

[redacted]

....

(Chairman, Graduate Council)

TABLE OF CONTENTS

LIST OF TABLES

LIST OF FIGURES

INTRODUCTION

As early as 1939 T. C. Barnes (1) observed that the electrical potential across frog skin is reduced when hyperosmotic solutions bathe the epidermal surface. More recently, investigators (2,3,4,5) have shown that the electrical resistance of the skin decreases as well as the electrical potential. Further, these investigations have shown that these decreases result from an increase in the passive flux of both sodium ions and several anions (2,4,5). As a result the net influx of Na^+ due to active transport is reduced by hyperosmotic solutions on the outer surface.

It wasn't until 1966 that Ussing (5) reported another interesting effect of hyperosmotic solutions on transport. He noticed that a net influx of sucrose occurred when the Ringer's solution bathing the outside of the frog skin was made hyperosmotic with 200 mM urea. This is in contrast to the situation with Ringer's solution bathing both sides of the skin, where the outflux and influx of sucrose are equal.

A common way of expressing the relationship between the directional fluxes across membranes is by the flux ratio which relates the influx to the outflux as:

$$\text{Flux Ratio} = \frac{\text{Influx (flux of solute from the outside bathing solution to the inside)}}{\text{Outflux (flux of solute from the inside bathing solution to the outside)}} \quad (1)$$

When the two directional fluxes for solutes such as urea or sucrose are equal, as is the case when Ringer's bathes both surfaces

of the frog skin, the flux ratio is equal to 1.0. When the influx is greater than the outflux the flux ratio is greater than 1.0 and when the influx is less than the outflux the flux ratio is less than 1.0. Ussing showed that when the outer bathing solution was made hyperosmotic with urea, the flux ratio for sucrose was greater than 1.0 in spite of the fact that a chemical gradient for the sucrose did not exist.

It appeared to Ussing that there was a positive correlation between the capacity of the skin to actively transport sodium ions from the outer bathing solution to the inner solution and the rate of net sucrose influx. Furthermore, Ussing was convinced that the anomalous transport of sucrose could be inhibited by poisoning the frog skin with cyanide. He therefore concluded that the hyperosmotically induced asymmetric movement of solute occurred as a result of a loss in the selectivity of the active sodium transport mechanism. He felt that the hyperosmotic urea solution acted to destroy the selectivity barrier of the transport mechanism and consequently to allow the sucrose to be actively transported from the outer to the inner bathing solution.

About this same time Franz and Van Bruggen (7) found that hyperosmotic solutions of solutes other than urea were capable of producing asymmetric movement of solute in an inward direction. Since there was an apparent increase in the asymmetry of the flux with increasing permeability of the hyperosmotic agent and increasing size

of the solute, these investigators discounted participation of any active transport mechanism and postulated that the asymmetry of the observed fluxes might result from an interaction between the diffusing hyperosmotic solute and the second tracer solute.

Later, Franz, Galey and Van Bruggen (8) further excluded participation of the active sodium transport system by showing that the asymmetry of the osmotically induced fluxes is not destroyed when the frog skin Na^+ transport system is inhibited by cyanide, dinitrophenol (DNP) or ouabain.

Biber and Curran (9) have subsequently shown that the solute flux is not altered by inhibition of sodium transport with ouabain or by replacement of all Na^+ in the Ringer's bathing solution by choline. They have shown further that no significant correlation exists between the movement of the asymmetrically moved tracer, mannitol, and the active sodium flux in toad skin. Biber and Curran concur with the suggestion that the asymmetric transport is the result of a coupling between the flows of the hyperosmotic agent and the driven solute.

As W. D. Stein (10) has stated, the only possible forces which can drive a net flux of a solute are: 1) the electrochemical gradient of the solute, 2) an interaction of the solute with an energy producing reaction, i.e., active transport, or 3) the interaction with the flux of some other component.

Since the work of Franz, Galey and Van Bruggen (8) and Biber

and Curran (9) has eliminated the possibility of the participation of active transport and since there is no known electrochemical gradient for the asymmetrically driven solute across the frog skin, it is evident that a coupling of flows exists between one solute and some other solute for which there is a chemical gradient.

This thesis will show that asymmetric solute transport can be produced across non-biological, synthetic membranes under conditions analogous to those described in the studies of frog skin. It will further be shown that the asymmetric flux of the driven solute is due to a coupling between the flow of the diffusible hyperosmotic agent and the driven solute.

It will also be shown that the nature of the "solute drag", as it will be called, is consistent with a mechanism involving frictional interaction between the two solute species in a porous membrane.

Background

One of the fundamental requirements of living cells is the maintenance of an acceptable internal environment to insure the proper function of biochemical processes. Teleologically speaking, nature has found encapsulation of constituents within a cellular or plasma membrane to be a simple but effective means of maintaining this requirement. The presence of such a barrier about the cell constituents gives the cell a measure of predictable composition and buffers the cell contents from the dynamic changes in pH, ionic

strength and solute concentrations constantly occurring in the interstitial fluids bathing the cell. These same cell membranes, however, must provide for the transport of metabolites into the cell and make it possible for metabolic wastes to be eliminated. The environment of the internal milieu must also be controlled by processes mediated by the cell membrane. Furthermore, a variety of cell products such as the endocrine products and exo-enzymes must be transported out of the cell through the plasma membrane.

The transport of solutes in biological systems has, however, a much broader concern that just the maintenance of the internal environment of the cell. Some tissues such as the capillary endothelium and intestinal mucosa function to move materials from one part of the organism to the other (11,12). Neural and muscular tissues utilize ionic transport to do work by creating electrical potentials (13). In addition, solute transport in the kidney and sweat gland is used to create osmotic flows of water which carry out the functional operations of the respective organs (14,15). Hence, solute transport across biological membranes plays an important role in the maintenance of life at the cellular, tissue, organ and organism levels.

The movement of solutes across biological membranes is known to take place by three different routes, namely: 1) direct passage through the lipoprotein membrane matrix (16), 2) pinocytosis and phagocytosis (17,18) and 3) transport through pores in the membrane (19,20).

Lipid-soluble substances may cross the cellular membrane by simply dissolving in the lipoprotein matrix of the membrane itself. In general, the transport of such lipophilic materials is dictated by the partition coefficient of the solute for the membrane constituents (21). The greater the partition coefficient or solubility in the membrane the greater the rate of transport of the solute.

It is thought that organic solutes and dissolved gases are the only substances transported by direct passage since these are the only solutes which have a large enough lipid-to-water partition coefficient to dissolve in the membrane (21). However, there is good evidence (22,23,24) that a substance which normally is not transported by direct passage may pass through the membrane if it can combine with a molecule within the membrane which acts as a "carrier". Such carrier molecules are thought to be free to move within the confines of the membrane and thus are able to associate with the transported solute on one side of the membrane and release it on the other side. By this process, called facilitated diffusion, solutes having low partition coefficients in lipids may be transported directly through the membrane (22).

Another mechanism by which solutes may cross cellular membranes is that of pinocytosis (17,18). In this process the transported solute is encapsulated by an invagination of the cell membrane. Pinocytosis appears to be an excellent mechanism by which large solutes may be transported, since the weight and dimensions of such molecules

would make solubilization or diffusion through the membrane difficult. It is not known to what extent this process is used in the transport of electrolytes and other small molecules.

The final mode by which solutes may cross a membrane is by passage through pores or holes in the membrane matrix. The ease of transport through such pores is largely dependent upon the size of the solute in relation to the size of the pore rather than to a property such as solubility in the membrane constituents. Indeed, it has been shown for many biological membranes that small molecules pass through cell membranes much more rapidly than larger solutes (19,25). These observations suggest the existence of pores in the membrane structure. Other evidence for the existence of porous membranes has also been presented by Ussing (3,20) and others (19,26,27) primarily by comparison of diffusive water flow to hydrostatic water flow and by the existence of solvent drag.

The Physical-Chemical Nature of Transport

The rate at which a substance crosses a membrane is a function of two factors. The first, which has just been discussed, describes the ease with which a solute moves through the membrane. This factor may be determined by the partition coefficient of the solute for the membrane, the affinity of the solute for a carrier, or by the size of the solute in relation to the number, size and shape of the pores through which it can pass. Secondly, the rate of transport is dependent upon the magnitude of the force or forces acting on the solute to

produce a directional flow.

The concept of the existence of two terms as regulators of solute transport is expressed well by a form of the Fick (28) equation modified to describe diffusion across a membrane of unknown thickness.

$$J_D = -P\Delta C \qquad (2)$$

This equation describes the flux, J_D, resulting from the diffusion of a solute down its concentration gradient. Here P, called the permeability coefficient, is the intrinsic term quantitating the ease with which the solute moves across a unit area of membrane. ΔC, the concentration difference across the membrane, is an extrinsic term describing the force on the solute created by the concentration gradient of the solute. Hence, diffusive flow is determined by two factors, one quantitating the ease of penetration and the second the force available to drive the solute.

In order to fully understand how solutes move across biological membranes it is important to know the source and nature of the driving forces behind the transport processes. We shall now look at how such forces might arise and how they might produce the movement of solutes.

One source of a driving force, or chemical potential, arises from solute concentration differences between the two phases separated by the membrane. A common form of solute movement across membranes

arising from such concentration differences is seen above in the example of the process known as diffusion. In diffusion, a solute having a concentration gradient moves down this gradient to the phase of lower concentration, i.e., lower chemical potential.

Concentration differences across a membrane may also result in the creation of an osmotic force capable of causing a flow of solvent into the more concentrated solute solution. It has been shown (29,30) that this osmotic flow of solvent can produce an asymmetric flow of solute from the solution of lower osmotic pressure into a solution of higher osmotic pressure. This process is known as solvent drag and will be discussed later in greater detail.

A second source of energy which may be used in the translocation of solutes is the metabolic activity of the cell. In the process known as active transport chemical energy of the cell is utilized to move a solute from one side of a membrane to another. Recent investigations (31,32,33) indicate that sodium-potassium transport processes may be related to the activity of sodium and potassium activated ATPase enzyme systems. While the mechanisms of such active processes are still speculative, it has been well established that active transport is an extremely important process, particularly in the control of the ionic environment of the cell (34).

The third source of energy for doing the work of solute transfer across biological membranes is electrical in nature. The

separation of positively charged particles from their anionic counterparts, by active transport or other processes (35), creates an electrical potential across the membrane. This potential can exert a force on the counter ion to move it from one side of the membrane to the other so as to reduce the electrical potential.

Thus, there appear to be three primary sources of energy for the movement of solutes across membranes: 1) concentration gradients, 2) electrical gradients, and 3) energy producing reactions within the cell, i.e., active transport. The interrelationships between these three sources of energy are complex and the importance of any one energy source varies from one situation to another as well as from one cell type to another.

The studies which are described in this thesis deal primarily with transport processes arising from concentration differences of nonelectrolytes across inert porous membranes. As a consequence, the investigations are not directly involved with active transport or electrical gradients.

Concentration-Dependent Transport Mechanisms

The force of diffusion is exerted by the random motion of molecules which tends to minimize the chemical potential of a solute by dispersing it uniformly throughout the solution (36,37,38). Thus a solute will diffuse from a center of high concentration to one of low concentration even if it is separated by a membrane, provided the membrane is permeable to the solute in question. As early as 1855

Fick (28) postulated what is now known as Fick's First Law of Diffusion. This law states that the rate of diffusion of a solute, i, across a barrier or reference plane may be described by,

$$\frac{dn_i}{dt} = -D_i(A)\frac{dC_i}{dx} \qquad (2a)$$

$\frac{dn_i}{dt}$ expresses the rate at which solute i crosses the plane of reference or membrane. D_i is the diffusion coefficient of the solute i and A is the area of the surface available for diffusion. $\frac{dC_i}{dx}$ is the concentration gradient of species i across the plane of reference of thickness X_i.

Since the amount of solute i which will cross the membrane per unit time, $\frac{dn_i}{dt}$, is the flux of solute i, X A, it is evident that Fick's First Law, equation 2a, may be written in terms of J_i, see equation 2.

When the membrane is permeable to the solvent but not to the solute, the concentration gradient expresses itself in the process called osmosis. While the nature of the force causing osmosis is not yet completely resolved (39,40) it is clear that osmosis is also the result of the solute gradient across the membrane.

In osmosis, the solvent, usually water in the biological systems, moves from the side having the lower solute activity into the solution of higher solute activity. The magnitude of the force produced by such a solute gradient may be measured by determining the

pressure that must be applied to the solution on the side having the higher solute concentration to block the flow of solvent into that solution. This pressure is known as the osmotic pressure of the solution.

Van't Hoff (41) showed in 1877 that for perfect, semipermeable membranes which allow solvent but not solute flow, the osmotic pressure created may be described by

$$\Pi = \Delta CRT \qquad (3)$$

where Π = the osmotic pressure difference across the membrane

ΔC = the difference in solute concentration across the membrane

R = ideal gas constant

T = temperature in degrees Kelvin

Few biological membranes are perfectly semipermeable, that is, they allow some solute to pass through their matrix. This tendency for the solute to move down its concentration gradient decreases the observed osmotic pressure from that pressure calculated by the Van't Hoff equation above, equation 3. The ratio of the observed osmotic pressure to the predicted pressure exerted across a perfect semipermeable membrane is known as the Staverman reflection coefficient, σ (42). The observed osmotic pressure exerted across a "leaky" membrane is expressed by equation 4.

$$\Pi_o = \sigma \Delta C_s RT \qquad (4)$$

As is apparent from 4, when $\sigma = 1$ the membrane is not permeable to the osmotic solute and the measured osmotic pressure is

equal to that predicted by equation number 3. However, when sigma is less than one, some solute may penetrate the membrane and the observed osmotic pressure is less than the theoretical osmotic pressure. When $\sigma = 0$ there is no osmotic pressure created by the solute since there is no selectivity of the membrane between the solute and solvent.

As mentioned earlier, the osmotic flow of solvent across the membrane into the hyperosmotic solution has been shown to be capable of creating a flux of solute into the hyperosmotic solution (29,30). This phenomenon, known as solvent drag, occurs when a solute, having a reflection coefficient of less than one, is found in the solution opposite to that having the hyperosmotic solution. The bulk osmotic flow of solvent through the membrane is said to "drag" with it the solute which has no inherent chemical potential for crossing the membrane. In reality a fraction of the chemical gradient of the solvent is imparted to the dragged solute. In this way the flow of the solvent and the flux of the solute are said to be "coupled".

It is the purpose of this thesis to present evidence for the existence of yet another mechanism by which solutes may be transported by the force created by differences in solute concentration across a membrane.

This phenomena will be referred to as "solute drag" and depends on both the hyperosmotic solute and a second solute which is

asymmetrically moved, both having reflection coefficients less than unity. It will be shown that a solute which has a concentration gradient across the membrane, but is also permeable to that membrane, can influence the movement of a second solute that has no chemical potential of its own for crossing the membrane. In this process, as distinguished from solvent drag, a coupling of flows exists between the flows of the two species rather than between the solvent and solute flows.

Nonequilibrium Thermodynamics

In any attempt to understand and elucidate mechanisms underlying scientific phenomena, it has been found useful to describe processes quantitatively in terms of kinetic equations. Such equations not only present a formal expression of the phenomenon, but aid in formulating a visual descriptive explanation of the process. However, there often arise situations in which the limited information available prevents the development of a kinetic description. It is at such times that scientists have turned to the formalism of thermodynamics. Although thermodynamics is unable to predict or rarely even suggest the mechanism by which a process takes place, it provides a formality of expression which is divorced from specific models. In this way classical thermodynamics has made it possible for investigators to learn more about the basic nature of processes underlying chemical and physical reactions. Classical thermodynamics, however, is only useful in describing systems at equilibrium or undergoing

reversible processes. Since biological systems are for the most part irreversible, open systems in which equilibrium is seldom, if ever, achieved, classical thermodynamics may play only a minor role in describing the processes taking place in living organisms.

However, the development of irreversible thermodynamics within the last decade has made it possible to formalize the non-equilibrium biological systems in a quantitative manner.

The basic principle of nonequilibrium thermodynamics is that any process can be considered as resulting from a force or forces acting to create a flux of matter, whether this matter be heat, energy, volume, mass, etc. The force which produces a flux, J_i, is known as the conjugate force of that flux and may be expressed as X_i. De Groot (43) has shown that under certain conditions the rate of entropy production, $\frac{dS}{dt}$ is equal to the sum of the products of the fluxes and their conjugate forces, i.e.,

$$\frac{dS}{dt} = \sum_i X_i J_i \qquad (5)$$

Since irreversible processes by their very nature produce entropy (44) the measurement of the rate of entropy production becomes a useful measure of the rate of the process being studied.

Although nonequilibrium thermodynamics as developed by Onsager (45), De Groot (43) and others (46,47) has been available for some years, it has only recently been applied to biological processes (23,28,49,50,51,52).

Kedem and Katchalsky (48,49) have applied irreversible thermodynamics to the processes of membrane permeation. In doing so they selected two mass transfers which describe the permeation of membranes. The total volume flow across the membrane is denoted by J_v and represents the flow of solute and solvent together. J_D is the symbol used to denote the flow of the solute relative to the flow of solvent.

The conjugate force of the flux J_v, i.e., the force producing the flow of solute and solvent together is the difference in pressure across the membrane and is denoted by Δp.

The term $RT\Delta C_s$ is the conjugate force which is responsible for the relative flow of solute and solvent, J_D. It should be apparent that this term is analagous to the osmotic pressure equation of Van't Hoff. See equation 3.

Kedem and Katchalsky in their 1958 paper (48) showed that the rate of entropy production for the transport of a solute across a membrane is given by the sum of the products of these fluxes and their conjugate forces. Thus,

$$\text{rate of entropy production} = \frac{dS}{dt} = J_v\Delta p + J_D\, RT\Delta C_s \qquad (6)$$

In order to write equations relating the conjugate forces to their resulting fluxes proportionality constants called phenomenological coefficients are used. The phenomenological coefficient Lp relates the pressure difference across a membrane Δp, to the observed

volume flow, J_V. The resulting equation at zero concentration difference across the membrane is expressed as

$$J_V = L_p \Delta p \tag{7}$$

Similarly, J_D, the relative velocity of solute to solvent, is related to its conjugate force, $RT\Delta C_s$, by the phenomenological coefficient, L_D, at zero pressure difference across the membrane. Thus,

$$J_D = L_D \, RT\Delta C_s \tag{8}$$

If a pressure difference, Δp, is created across a membrane, equation 7 states that a volume flux, J_V, will result. The magnitude of this J_V for any one pressure difference is determined by the coefficient Lp. If the solution being forced through the membrane by Δp contains a solute that is not permeable to the membrane, the solute will be excluded by the membrane. This filtration creates a flow of solute relative to the solvent or J_D. Hence a new coefficient must be introduced which relates Δp to J_D. Such a term which relates a force to a flow other than its own primary flow is called a cross-coefficient or a cross-term coefficient. The cross-coefficient which is caused by the process just described is often called the ultrafiltration coefficient and is denoted by L_{Dp} or L_f.

Analagously, if a solute concentration difference is created across a membrane, a net volume flow, J_V, results from osmosis.

The cross-coefficient in this case is called the osmotic coefficient and is denoted by L_{pD} or L_D. Furthermore, it has been shown by Staverman (53) that the ratio of the osmotic coefficient, L_{pD}, or ultrafiltration coefficient, L_{Dp}, (since they are equal - see equation 11) to L_p, the hydraulic conductivity coefficient, is equal to the reflection coefficient σ. Hence,

$$\sigma = \frac{-L_{pD}}{L_p} = \frac{L_{Dp}}{L_p} \tag{9}$$

Now that we have defined the possible sources of force capable of creating flows, it should be possible to write flux equations which take into consideration both direct and cross phenomena. Consider first the total volume flow across a membrane, J_v.

If a cross-coefficient, L_{pD}, is significant, we see that J_v arises from differences in ΔCRT across a membrane as well as differences in hydrostatic pressure, Δp, and a formal statement of volume flow as derived by Kedem and Katchalsky as:

$$J_v = L_p \Delta p + L_{pD}\, RT \Delta C_s \tag{10}$$

Onsager postulated in what is known as the Onsager Reciprocal Relation Theorem that "If the proper choice is made of the fluxes and forces then the cross-coefficients will be equal" (45). The proper choice of fluxes turns out to be one in which the sum of the products of each force and its conjugate flux is equal to the rate of

entropy production in the irreversible process considered (43). Thus Kedem and Katchalsky's choice of fluxes and forces insure that these conditions are satisfied.

This means that,

$$L_{pD} = L_{Dp}. \tag{11}$$

As is obvious, these two cross-term coefficients are related to the interaction between solute and solvent. Ginzburg and Katchalsky (30) as well as Ussing (29) have shown that the amount of interaction between solute and solvent is biologically significant in creating sizable solute flows when solvent flow across a membrane is present. This phenomenon, as we have previously mentioned, is known as solvent drag.

The total flux of solute may be written as the sum of fluxes which are responsible for the movement of solute. Hence, in terms of the two fluxes, J_v and J_D which have just been described, J_s, the total rate of flow across the membrane, can be written as

$$J_s = (J_v + J_D)\ C_s \tag{12}$$

The sum of $J_v + J_D$ gives the total volume flow for that part of the solution occupied by the solute. Since it is more convenient to measure and express the rate of flow of solutes in terms of moles of solute crossing the membrane rather than in terms of

volume of solute crossing, we multiply the sum $J_v + J_D$ by C_s, the concentration of solute in moles per unit volume. Hence J_s is expressed in moles of solute crossing the membrane in a given unit of time.

Using equation 8, 9, 10, 11 and 12 one can, with little difficulty, obtain the equation below, see Stein (54).

$$J_s = (1 - \sigma) J_v C_s + (L_D - \sigma^2 L_p) C_s \, RT\Delta C_s \tag{13}$$

The term $(L_D - \sigma^2 L_p)C_s$ can be experimentally measured and is given the symbol ω and this ω is called the permeability coefficient for the solute. Alternatively, $(L_D - \sigma^2 L_p)C_s$ RT can be replaced by P_s, also called the permeability coefficient. Below we see the expressions for ω and P_s and how the two are related. Since,

$$\omega = (L_D - \sigma^2 L_p)C_s \tag{14}$$

and

$$P_s = (L_D - \sigma^2 L_p)C_s RT \tag{15}$$

then dividing 15 by 14,

$$\frac{P_s}{\omega} = RT \tag{16}$$

and

$$P_s = \omega RT \tag{17}$$

Since P_s is also easily measured and includes the RT term not included in ω it is often the expression of choice.

We may now substitute ω or P_s into equation 13 which becomes:

$$J_s = (1-\sigma)\, J_v C_s + \omega RT \Delta C_s \qquad (18)$$

or

$$J_s = (1-\sigma)\, J_v C_s + P \Delta C_s \qquad (19)$$

Just as hydrostatic pressure can create a flux of solute relative to the solvent, necessitating the cross-term coefficient L_{Dp}, the movement of one solute, 1, may also influence the flux of a second solute, 2, necessitating the cross-term coefficient relating the effect of one flux of one solute on that of a second. The term P_{21} is the cross-term permeability coefficient which expresses the effect of solute 1 on the flux of solute 2.

If one desired to investigate the effect of one solute on the flux of a second solute, it is apparent that equation 18 or 19 would become much more formidable since new terms for the second solute would have to be considered. It is also quite possible that the $(1-\sigma)\, J_v C_s$ term, which is responsible for solvent drag, could mask any influence of the second solute which may be present.

To simplify the consideration of solute-solute interaction, it is apparent that it would be advantageous to reduce the total volume flow across the membrane, J_v, to zero. If this is done,

equation 6 reduces to

$$\frac{dS}{dt} = J_D \, RT\Delta C_s \tag{20}$$

and provided the total volume flow, J_v, is maintained at zero, equations 18 and 19 for the flux of a single solute, s, become

$$J_s = \omega RT\Delta C_s \tag{21}$$

or

$$J_s = P_s\Delta C_s . \tag{22}$$

In terms of P_s the equation describing the total flux of two different solutes, 1 and 2, diffusing simultaneously under the conditions of zero volume flow may be written as:

$$J_T = P_{11}\Delta C_1 + P_{22}\Delta C_2 + P_{12}\Delta C_2 + P_{21}\Delta C_1 \tag{23}$$

when $J_v = 0$

Where J_T = total solute flux

P_{11} = permeability coefficient of solute 1

P_{22} = permeability coefficient of solute 2

P_{12} = permeability coefficient of solute 1 induced by solute 2

P_{21} = permeability coefficient of solute 2 induced by solute 1

ΔC_1 and ΔC_2 are the concentration differences of solutes 1 and 2 across the membrane.

The first two terms, $P_{11}\Delta C_1$ and $P_{22}\Delta C_2$, are the normal expressions for the diffusion of a solute down its concentration gradient. $P_{12}\Delta C_2$ and $P_{21}\Delta C_1$ describe the solute fluxes of solute 1 created by the flow of solute 2 and the flux of solute 2 arising from interaction with solute 1, respectively. Only when there is coupling between the flows of the two solutes will P_{12} and P_{21} be different from zero.

Since in the present work it is desired to determine whether the flux of one solute, 2, can influence the flow of another solute, 1, it will be convenient to look at the effect of solute 2 on the total flux of solute 1 or J_1. The equation describing the total flux of solute 1 can be written as

$$J_1 = J_{11} + J_{12} \qquad J_v = 0 \qquad (24)$$

where J_1 is the total observed flux of solute 1, J_{11} is the diffusional flux of solute 1 alone, and J_{12} is the flux of solute 1 caused by the flux of solute 2. Remember that the fluxes we are concerned with at this time are those that take place in the absence of any volume flow, J_v, and in this case $J_s = P_s\Delta C_s$, equation 22. Hence equation 24 can be written:

$$J_1 = P_{11}\Delta C_1 + P_{12}\Delta C_2 \qquad J_v = 0 \qquad (25)$$

Rearranging equation 24 we see that the flux of solute 1 which is

due to solute 2 can be expressed by

$$J_{12} = J_1 - J_{11} \qquad J_v = 0 \qquad (26)$$

Since J_{11} is the flux experimentally observed when solute 1 is the only solute diffusing down its concentration gradient, the flux of solute 1 can be calculated by subtracting this value from the total flux observed when solute 2 is also present in the system.

Alternatively, if there is no concentration gradient for solute 1, that is $\Delta C_1 = 0$, the observed flux of solute 1 will be due to solute 2 interacting with solute 1. Hence,

$$J_1 = J_{12} = P_{12}\Delta C_2 \qquad (27)$$

Provided $J_v = 0$ and $\Delta C_1 = 0$.

Rearranging equation 27 we see that the cross coefficient, P_{12}, representing the effect of solute on the flux of solute can be expressed as

$$P_{12} = \frac{J_1}{\Delta C_2} \qquad (28)$$

where: $\Delta C_1 = 0$

$J_v = 0$

It is this P_{12} term which must be shown to be different from zero in order to show the existence of solute drag.

To quantitate the magnitude of the solute drag one can

divide the P_{12} term by P_{22}, the permeability of solute 2, diffusing across the membrane. In this way one may show the relative effectiveness of several number 2 solutes as a "driver" or "solute dragger" species (55,56). Hence,

$$\text{Effectiveness of interaction of solute 2 with 1} = \frac{P_{12}}{P_{22}} \qquad (29)$$

MATERIALS AND METHODS

Membranes

The experiments described here were carried out on four synthetic membranes differing in physical properties and composition. These membranes were the S & S B20 membrane, the Diaflow UM-3 ultrafiltration membrane, Union Carbide dialysis tubing, and the General Atomic Type B desalinization membrane. A number of the physical characteristics of these membranes are listed in Table I.

Initial studies were carried out on the Diaflow UM-3 ultrafiltration membrane, manufactured by Amicon Corporation, Cambridge, Massachusetts. It is an anionic, hydrated polymer ultrafilter which is thermally and dimensionally stable. The membranes are cast from mixtures of sodium polysodium styrene sulfonate and polyvinyl benzytrimethylammonium chloride (57). It is a "skinned" anisotropic membrane analogous to cellulose acetate membranes and consists of a "skin" about 1μ thick made up of consolidated layers of the polyelectrolyte complex. Beneath this skin are thick, spongy, opaque layers of the same polymers which give structural support to the barrier skin layer but offer little resistance to flow (57).

The Diaflow membranes show a hydraulic conductivity coefficient, Lp, of approximately 2.0×10^{-10} cm^3 $dyne^{-1}$ sec^{-1}. The procedure by which this coefficient is determined is described in this section of the thesis. The effective pore radius calculated from reflection coefficients of several different solutes by the

method of Goldstein and Solomon (19) gave values of approximately 120 Å while a second UM-3 membrane gave a pore radius of approximately 400 Å as measured by this method. Another method of estimating the effective pore radius which depends on the diffusive permeability of water as compared to the hydraulic conductivity measured by L_p was developed by Paganelli and Solomon (27). This method gives values of approximately 367 Å for the effective pore radius of the membrane, which is in good agreement with the value of 400 Å.

The second synthetic membrane investigated was the S & S B20 cellulose acetate membrane filter available from Carl Schleicher and Schuell Company, Keene, New Hampshire. As stated by the manufacturer, these filters "have an extremely uniform micropore structure (58) and are approximately 100μ thick." There is evidence (59) that cellulose acetate membranes are similar in structure to that of the polyelectrolyte membranes such as the Amicon membrane described above (57). Riley et al. (59) have shown by electron microscopy that cellulose acetate membranes have an extremely thin and dense surface skin overlying a much more porous and thick backing. It is felt that the dense skin layer is responsible for the filtration properties of the membrane (59) as it is for the Diaflow polyelectrolyte complex membrane (57). As seen in Table I, the B20 membrane shows a L_p of 0.66×10^{-10} cm^3 $dyne^{-1}$ $sec.^{-1}$ and an effective pore radius of approximately 80 Å or 70 Å as determined by the methods of Goldstein and Solomon and

Table I

Characteristics of Synthetic Membranes

		Dia-flo UM-3	S & S B20	GA Type B
1. Composition		Poly Electrolyte	Cellulose Acetate	Cellulose Acetate
2. Thickness (μ)		∿ 200	∿ 100	+
3. Effective Pore Radius (Å)	*A	∿ 300-350	∿ 80	∿ 20
	**B	∿ 370	∿ 70	∿ 25
4. L_p ($cm^3 dyne^{-1} sec^{-1}$)		2.0×10^{-10}	0.66×10^{-10}	1.3×10^{-10}

* By the method of Goldstein and Solomon (19)

** By the method of Paganelli and Solomon (27)

\+ Unknown

Paganelli and Solomon, respectively. Considering that each method is based upon different parameters of membrane permeability the agreement between the values obtained is quite good.

The third membrane to be investigated as a desalinization membrane material produced by General Atomic Division of General Dynamics, San Diego, California. The material, designated Type B by the manufacturer, is a cellulose acetate membrane similar to the B20 membrane and shows an L_p of 1.3×10^{-10} cm^3 $dyne^{-1}$ sec^{-1}. The measured effective pore radius of material is 20 - 25 Å as determined by the method of Goldstein and Solomon and Paganelli and Solomon described in this section.

Solutes.

Solutes used in this work were urea, mannitol, sucrose, raffinose, inulin and dextran. Table II presents a compilation of the molecular dimensions for these solutes as determined by a number of investigators. In general, the dimensions of the solutes determined from diffusion studies are used in the calculations of this thesis since most of the present studies are closely related to diffusion.

Reagent grade urea and sucrose were obtained from Merck and Co., Inc., Rahway, N. J. In most experiments 0.35 molal solutions

Table II

Molecular Dimensions of Solutes

Solute	Determined from Diffusion Measurements					Determined from Viscosity Measurements				
	half axis of ellipse Å		Ref.	r of equivalent sphere r(Å)	Ref.	half axis of ellipse Å		Ref.	r of equivalent sphere r(Å)	Ref.
	a	b				a	b			
DHO	-	-		1.9	(72)	-	-		-	
Urea	-	-		2.7	(72)	-	-		-	
Mannitol	3.6	3.6	(26)	4.4	(72)	5.0	3.2	(26)	3.8	(26)
Sucrose	4.4	4.4	(26)	5.3	(72)	8.3	3.4	(26)	5.0	(26)
Raffinose	7.5	4.7	(26)	6.1	(72)	8.2	4.4	(26)	5.7	(26)
Inulin	4.0	6.3	(26)	1 5	(26,+)	35.2	6.7	(26)	15.3	(26)
Dextran										
Hydrolysates										
$15x10^3$ MW	100	6	(86)							
$84x10^3$ MW	290	8.5	(86)							

+ Calculated from equation of Durbin (72)

of these solutes were used and each showed osmotic pressures, as measured by freezing point depression, of ∿354 ± 12 milliosmoles. Mannitol and raffinose were obtained from Matheson Coleman and Bell division of the Matheson Company Inc., East Rutherford, N. J. Both solutes show melting points which agree with those of the pure substances (60). 0.35 molal solutions of these solutes have measured osmolarities of 350 ± 7 and 357 ± 10 milliosmoles respectively as determined by freezing point depression.

Dextran (Type 15) obtained from Sigma Chemical Company was stated by the supplier to have an average molecular weight of 19,900. Fifteen percent solutions of this dextran preparation were used but osmotic pressures could not be measured accurately by freezing point depression (61).

Inulin was not used as a hyperosmotic solute due to its low solubility in water.

All of the above solutes were checked for purity by paper chromatography. Each solute migrated as a single spot and showed Rf values characteristic of the solute in the given solvent system. Procedures used in the chromatography of both labeled and unlabeled solutes are described later.

Radioactively labeled solutes were used to measure permeability coefficients in the studies of solute fluxes. For such studies, isotopic purity of the tracer is essential. If the tracer is contaminated with a small, more permeable solute, the P value

calculated for the solute flux will not be the true value of the tracer of interest but will also reflect the greater permeability of the contaminant. Similarly, if the tracer is contaminated by a significant amount of another larger labeled solute less permeable than itself, the P value determined will be lower than the true permeability coefficient of the pure tracer solute. These discrepancies arise because P values are determined by using the radioactivity on the "donor" side of the membrane as a reference to which the amount of radioactivity crossing the membrane is compared. This calculation is based on the premise that the radioactivity on the donor side represents the labeled solute species which has crossed the membrane. If this assumption is not true, the P value calculation is invalid as a measure of flux for the single solute. Consequently, care was taken to assure the absence of radioactive contaminants. Since carbohydrates are quite vulnerable to hydrolysis and attack by microorganisms, particular care was taken to detect the presence of any hydrolysis or metabolic products.

^{14}C labeled urea, New England Nuclear Corp., Boston, Mass., was dissolved in distilled water and purged with CO_2 to drive off $^{14}CO_2$ which may have contaminated the solute.

Crystalline D-mannitol-1-^{14}C, obtained from Nuclear Research Chemicals Inc., Orlando, Florida, was dissolved in distilled water and diluted to a known volume. An aliquot of this solution was acidified with HCl to a pH of 3.0. This acidic solution was then warmed, shaken, and the atmospheric pressure reduced to remove $^{14}CO_2$. NaOH

was added to obtain a pH of 8.4 and the solution diluted to a known volume. An appropriate aliquot was radioassayed in the Packard 3000 Liquid Scintillation Spectrometer using the Buhler ethanol-toluene liquid scintillation media (62). It was found that there was no real loss of radioactivity during the acidification procedure, hence a negligible amount of $^{14}CO_2$ was present in the mannitol solution. An aliquot of the dilution was assayed for $^{14}CO_2$ by the micro CO_2 determination of Van Bruggen and Scott (63) which showed no $^{14}CO_2$ to be present. Chromatography of this mannitol is described later. Mannitol-1-^{14}C obtained from New England Nuclear Corp. was received in 70% ethanol. This solution was taken nearly to dryness by gentle heating on a steam bath in a stream of N_2 and then quantitatively transferred and diluted to a known volume with distilled water. After warming and allowing to stand the solution was purged with CO_2 to remove $^{14}CO_2$.

Uniformly labeled sucrose-^{14}C was also assayed for $^{14}CO_2$ by the method of Van Bruggen and Scott (63) and was shown to contain negligible amounts of $^{14}CO_2$. As a precautionary measure all ^{14}C labeled sucrose received was purged with CO_2 before use.

Since neither ^{14}C or ^{3}H labeled raffinose was commercially available it was necessary to prepare and purify ^{3}H raffinose. The method of labeling raffinose chosen was the Wilzbach reaction (64, 65) in which the solute to be labeled is sealed in an ampoule with carrier-free tritium gas. Two hundred milligrams of raffinose was

so treated by the Wilzbach reaction for two weeks under an atmosphere of 3 curies of tritium gas by the New England Nuclear Corp., Boston, Mass. The product, approximately 1/8 of which was labeled raffinose, was purified by Dr. Harriet Frush of the National Bureau of Standards using descending paper chromatography in a n-butanol-pyridine-H_2O-benzene (50:30:30:4.5) solvent system on Whatman No. 17 paper. The labeled material thus purified migrated at the same Rf as cold raffinose in two different solvent systems with descending paper chromatography.

Inulin-carboxyl-^{14}C and inulin-methoxy-^{3}H were obtained from New England Nuclear Corp., Boston, Mass. The ^{14}C labeled inulin contained little or no $^{14}CO_2$ as shown by assay before and after purging solutions of the solute with CO_2. Column chromatography of inulin-carboxyl-^{14}C on Sephadex G 75 showed better than 95% of the radioactivity to be in a single peak as shown in Fig. 1. Likewise, inulin-methoxy-^{3}H showed a single peak on Sephadex G 75 chromatography with 100% of the activity in that peak (Fig. 2). It is significant that the elution volumes of ^{14}C and ^{3}H labeled inulin are essentially identical.

^{14}C labeled dextran of two molecular sizes were obtained from the New England Nuclear Corp. These dextran hydrolysates were stated by the supplier to have molecular weights of 16,000-19,000 and 60,000-90,000. Both fractions were supplied as carboxyl-^{14}C dextran. Solutions of these solutes were purged with CO_2 before use to eliminate

Figure 1

Elution profile of carboxyl-^{14}C-inulin on a Sephadex G 75 column. The bed dimensions were 1.5 x 90 cm, the flow rate was 1 ml per 7 min., and the applied sample size was 1 ml. The solvent for the sample and the eluant was 0.1 M NaCl.

Figure 2

Elution profile of methoxy-^{3}H-inulin on a Sephadex G 75 column. The bed dimensions were 1.5 x 90 cm, the flow rate was 1 ml per 7 min., and the applied sample size was 1 ml. The solvent for the sample and the eluant was 0.1 M NaCl.

The similarity of the two inulin elution profiles made it possible for either ^{14}C or ^{3}H inulin to be used as tracer solutes.

Figure 1

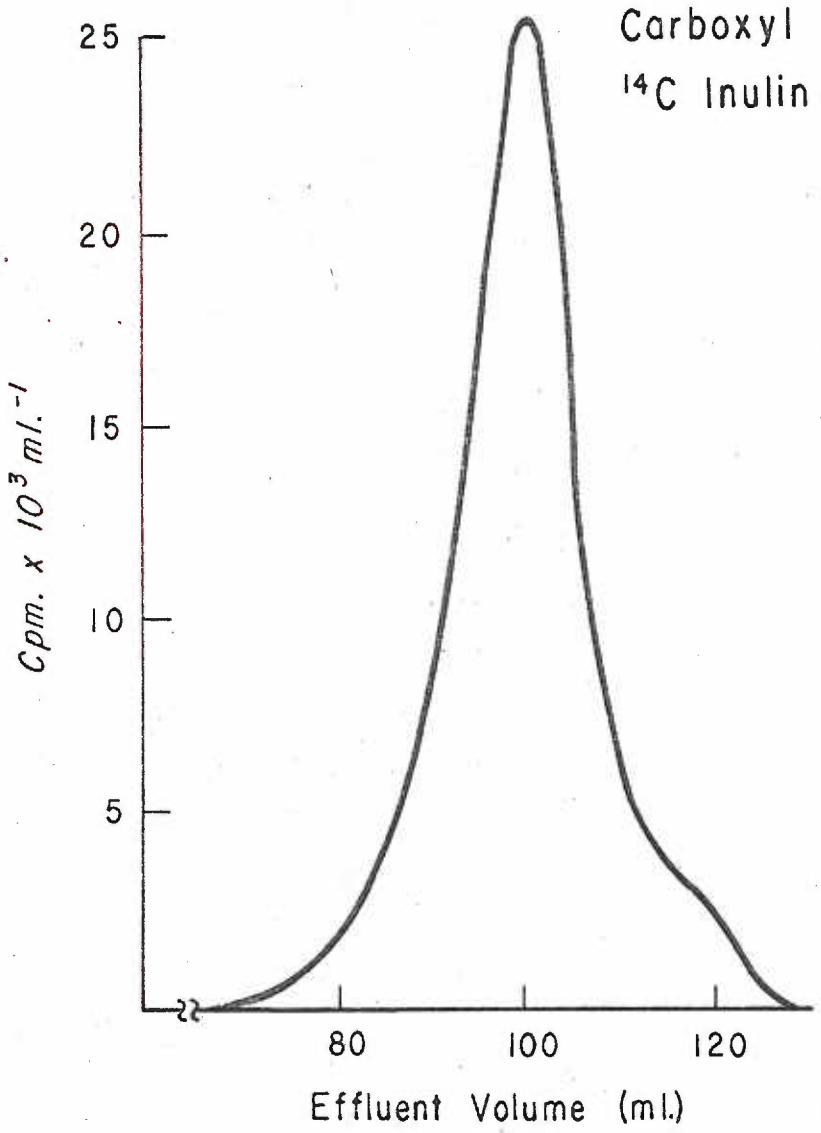

Figure 2

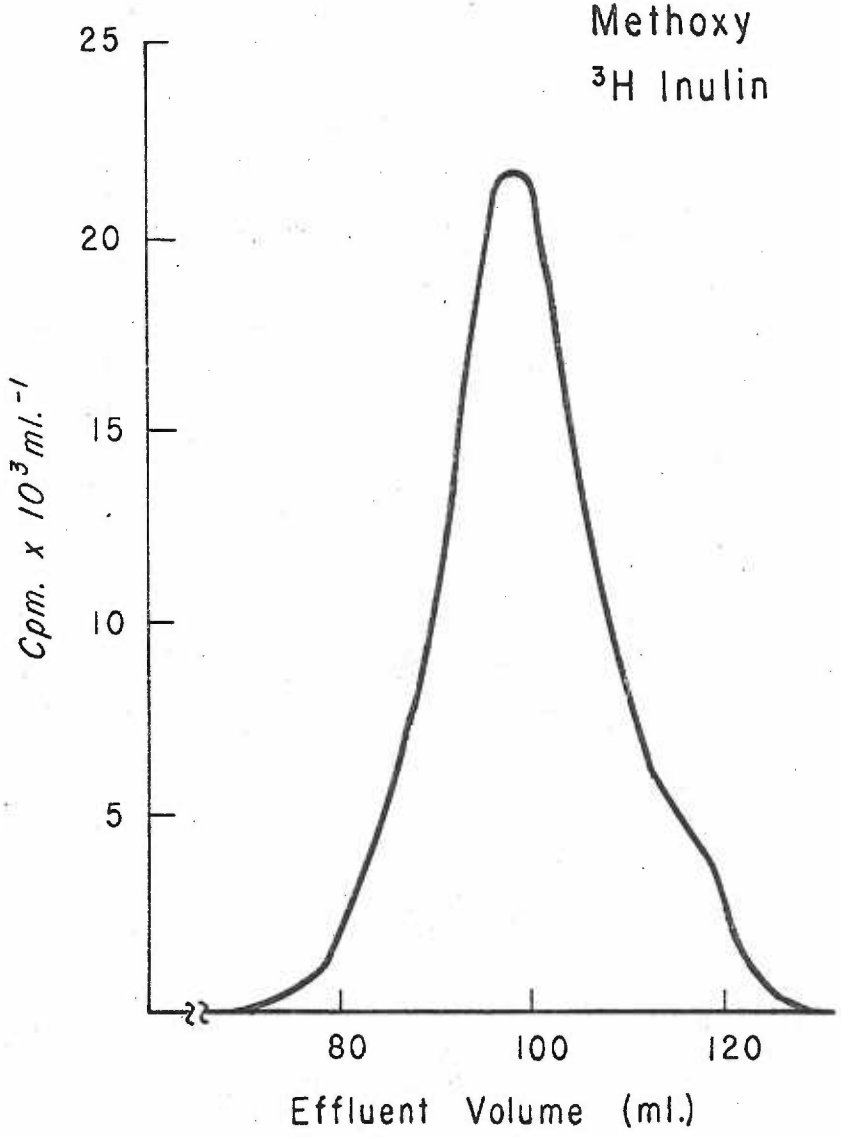

$^{14}CO_2$ contamination.

Paper Chromatography of Solutes

All of the solutes used in the studies were chromatographed as a measure of the purity. The solvent system was butanol, pyridine, benzene and H_2O 50:30:4.5:30 (66). Descending paper chromatography was carried out on Whatman #3 paper for approximately 18 hours. The radioactively labeled specie of each solute was run with and without unlabeled solute as carrier and unlabeled solutes were also run in the same system. The location of the radioactive material was determined by scanning the chromatogram with a Nuclear Chicago Actograph II strip scanner and the location of non-labeled solutes was determined by staining the chromatograms with 0.002% sodium meta periodate and 2% p-anisidine in 5% glacial acetic acid (67). In all cases the Rf values of the radioactively labeled material corresponded to that of the non-labeled solute. All solutes tested traveled as a single band and showed no evidence of contamination. The Rf's of the solutes used in the studies are shown in Table III along with glucose, a constituent common to sucrose, raffinose and dextran. None of these three solutes showed any contamination of glucose. Hydrolysis products of dextran and inulin such as glucose and fructose definitely show rates of migration different from those of the parent compounds. In no instance were indications of these hydrolysis products seen in chromatography of inulin or dextran.

Table III

Rf Values of Solutes*

Solute	Rf
Mannitol	0.36
Sucrose	0.30
Raffinose	0.17
Inulin	0.05
Dextran I	
MW ($16 - 19 \times 10^3$)	0.05
Dextran II	
MW ($60 - 90 \times 10^3$)	0.05
Glucose	0.38

*In system of 50:30:4.5:30 butanol-pyridine-benzene and water on Whatman #3 paper.

Osmotic Pressures of Solutions and Experimental Procedures

Osmotic pressures of solutions used in the studies were measured by freezing point depression on an Advanced Osmometer manufactured by Advanced Instruments, Inc., Newton Highlands, Mass.

Measurement of Solute Fluxes

Many of the experiments carried out consisted of the measurement of a flux of tracer solute across a membrane. The general procedure for such experiments is as follows: On one side of the membrane is placed a solution containing the radioactive tracer solute. To this is added unlabeled solute of the same compound to make the solution 1 millimolar for the solute. The opposite solution is also made one millimolar with the non-radioactive solute. After an initial equilibration period an aliquot of the formerly non-radioactive solution is taken by micropipette or syringe and an equal volume of non-labeled solution is replaced so that the volume of solution remains constant. Samples are taken continuously in this way, at regular intervals (usually 5 minutes) for from four to eight consecutive periods.

The permeability coefficients of solutes are determined by dividing the amount of radioactive tracer moving across a unit area of membrane in an interval of time by the concentration of the radioactive tracer in the donor solution. Hence P is a rate constant with the dimensions of $L \cdot T^{-1}$. A more detailed description of the calculations of P, which is also equal to the flux at unit concentration,

is given by Franz (68).

The radioactivity of the solutions is determined on either a Nuclear Chicago 1043 B low background gas-flow Geiger counter or a Packard Tri Carb series 3000 dual channel liquid scintillation spectrometer.

Samples are prepared for the low background counter by evaporation of the aliquot in a 1.25 inch diameter stainless steel planchet in which a lens tissue disc has been placed. In addition to the lens tissue 0.150 ml of a "glue" consisting of a H_2O solution of 5% glucose, 20% ethyl alcohol, and 0.05% Aerosol is added to the planchet prior to the sample. This glue solution fulfills the dual purpose of improving the spreading of the sample by decreasing the surface tension of the solution and "gluing" the solute to the lens tissue disc and steel planchet (69).

The majority of the radioactivity assays were done on the liquid scintillation spectrometer for which the samples are prepared in the following way. The sample to be assayed is added directly to 10 ml of scintillation fluid in special glass vials. The scintillation fluid used follows a recipe of Bray (70) and is composed of 60 gm napthalene, 100 ml absolute methanol, 20 ml ethylene glycol, 4.0 gm 2,5-diphenyloxazole (PPO), 0.2 grams 1,4 bis-2-(5-pheyloxazolyl)-benzene (POPOP) and dioxane in an amount to make the total volume up to 1 liter. In some solutions PPO and POPOP were replaced by 4 grams of Omnifluor (a blend of 98% PPO and 2% bis-MSB available from New

England Nuclear Corp., Boston, Mass.). To this solution was added 40 grams of Cab-o-sil available from Cabot Corporation, Boston, Mass. This material makes a thixotropic gel of the Bray's solution and has been found extremely useful in suspending insoluble solutes for liquid scintillation counting (71). This "Bray's Gel", as it is called, was used in the assay of most of the experiments.

Apparatus

Experiments were carried out in the apparatus shown in Figures 3, 4 and 5. Each membrane was mounted as a barrier between the two plastic chambers shown in Figs. 3 and 4. The membrane was supported between two flattened 20 mesh stainless steel screens held in parallel planes by metal rings. The cassette so formed is shown suspended between the open chamber halves in Fig. 4. The system is closed by wing nut-applied pressure, the seal between the stainless steel rings of the cassette and the chambers being made by Neoprene O-rings embedded in the faces of the chambers. The solutions bathing the membrane are stirred by small Teflon coated magnetic bars driven by external magnets mounted on 600 rpm synchronous clock motors available from Herbach and Rademan, Philadelphia, Pennsylvania. The chambers created by the seal of the plastic pieces to the cassette are filled or sampled through ports in the top of each chamber. These ports are sealed with disposable rubber closures, Critocaps J (Clay-Adams Inc., New York, N. Y.) and the closures are held in place by hollow threaded plastic plugs. The drain ports in the bottom of the

Figure 3

View of assembled chamber apparatus. On the right is seen the microburet apparatus used in measuring volume changes. Volume flows are determined by measuring the amount of solution which must be added or subtracted to maintain the fluid level in the glass capillary standpipe seen at the center of the photograph (see also Figure 4).

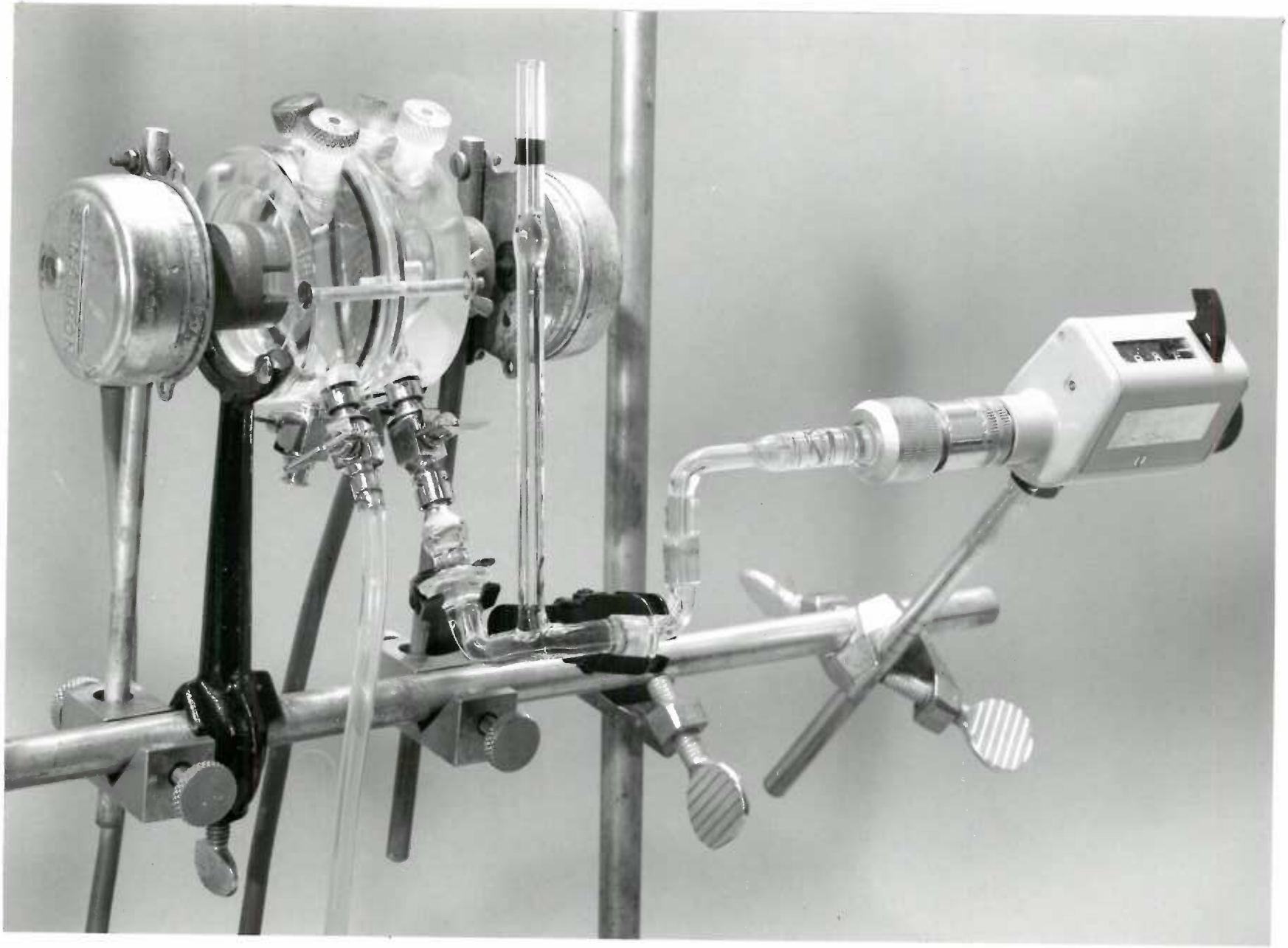

Figure 4

View of apparatus in expanded form. The membrane is held within the metal rings and restraining wire screens shown supported in the mid line of the figure. The chambers are made of plastic and are tapered so as to have a minimum volume. Teflon covered stirring bars are held against the back of the chambers and stirred by the 600 RPM timer motors fitted with magnets.

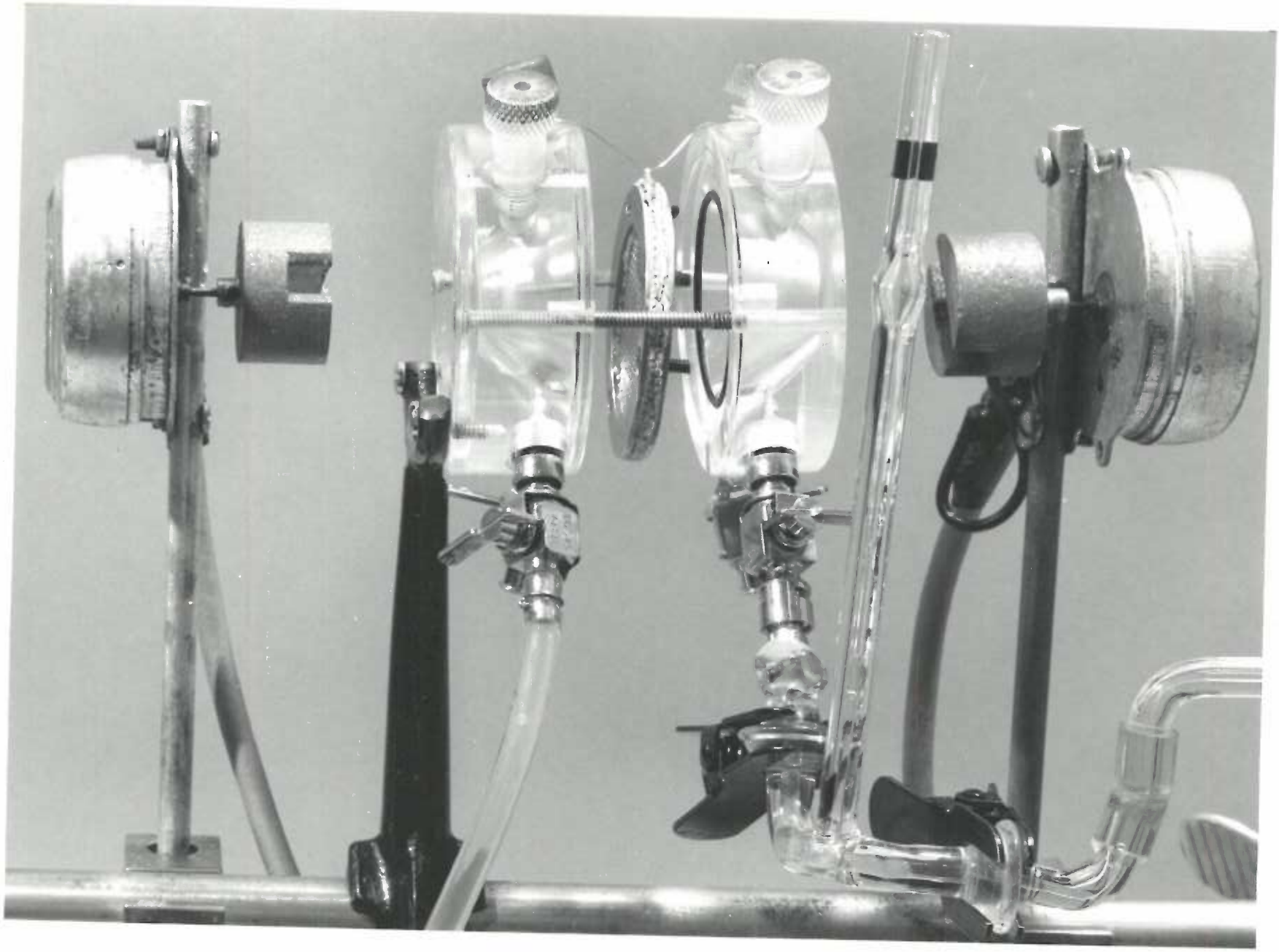

Figure 5

View of assembled apparatus showing the essential components. In the center is the assembled chamber, on the right the microburet used for measuring volume changes. The left side of the chamber is attached to a mercury pressure device for the imposition of pressures up to 2 atm. When greater pressures are needed the mercury device is replaced by a compressed gas cylinder and gauge arrangement.

chambers are sealed by metal stopcocks (Becton, Dickinson and Co., Rutherford, New Jersey).[1] The other two ports toward the front of the chamber may also be sealed by metal stopcocks and are used for the measurement of volume flow or the application of hydrostatic pressure.

The stopcock on the left chamber may be attached to a pressure device as seen on the left of the chamber assembly in Fig. 5. This mercury manometer device, developed for these studies, is used to apply hydrostatic pressure to the solution on the left hand side of the membrane. The pressure is attained by pumping air into the mercury reservoir by a hand operated bulb or by an air line and is measured by the height of the mercury column. Fine adjustment of the pressure is made by the displacement of a screw driven plunger in the barrel of a 10 ml syringe. An air tight seal between the barrel and plunger is made by a mercury reservoir seal fashioned at the top of the syringe barrel. In cases where pressures greater than 150 cm of mercury are used, an Ashcroft 100 pound per square inch test gauge, Industrial Air Products, Portland, Oregon, is used to measure the hydrostatic pressures.

To the stopcocked port on the right hand chamber is attached a glass capillary standpipe with a reservoir bulb and a reference marker corresponding to the top of the water level in the chamber.

[1]The metal stopcocks are joined to the chambers with the use of a cement (Dolphan CN-1065 Epoxy Adhesive, John C. Dolph Company, Monmouth Junction, New Jersey).

A ground glass ball-joint makes the connection between the standpipe and a modified micropipet-buret with automatic zeroing and digital readout (Manostat Digi-Pet 2464-U10, Arthur H. Thomas Co., Philadelphia, Pa.). The total capacity of the micropipet-buret is 1 ml and each division on the digital readout is equal to 0.2 µl.

The apparatus just described is used to measure volume flows across the membrane. To measure such flows the plunger of the micro-buret is either advanced or retracted to bring the water meniscus in the standpipe to the reference point marked on the standpipe. The amount of fluid added or removed from the system in order to maintain the level of the meniscus in the standpipe is the net volume flow across the membrane and is read directly from the micro-buret. In this way, volume flows across the membrane may be measured whether they occur from hydrostatic or osmotic pressure.

Determination of σ, the Reflection Coefficient

Reflection coefficients, or σ's, are important characteristics of a membrane since they can be used to determine the effective pore radius of the membrane (19). As described earlier, the reflection coefficient describes the effectiveness of the solute as an osmotic agent, a perfectly semipermeable solute having a reflection coefficient of 1.0.

The reflection coefficients of all the solutes used were found by determining the hydrostatic pressure necessary to block osmotic flow, in effect by measuring the osmotic pressure created by

a known concentration of the test solute. This observed osmotic pressure was used to calculate the reflection coefficient as:

$$\Pi_o = \sigma \Delta CRT$$

or (30)

$$\sigma = \frac{\Pi_o}{\Delta CRT}$$

The determination of the observed osmotic pressure Π_o is made by placing a solution containing a known concentration of the solute to be tested in the chamber on the left of the membrane. Distilled water is placed in the right hand chamber and the filling ports of both chambers are closed. Increasing amounts of pressure are then applied to the chamber containing the test solute until the osmotic pressure is balanced by the hydrostatic pressure and the net volume across the membrane is zero. The observed osmotic pressure is then used to calculate σ, the reflection coefficient.

A second method used to determine the reflection coefficient is based upon the ability of the solute tested to create osmotic flow. In this method use is made of the fact that the reflection coefficient is the ratio of the osmotic coefficient L_{pD} (or ultrafiltration coefficient) to the pressure filtration coefficient, L_p, as in the following:

$$\sigma = \frac{-L_{pD}}{L_p} \quad (31)$$

This relation described by Staverman (42) has been successfully used by Durbin (72) and Ginzburg and Katchalsky (30) as well as others. L_{pD} is determined in a manner similar to that used to determine the reflection coefficient above except that instead of blocking the osmotic water flow, that flow is measured for several periods of less than one minute. Since the osmotic flow of water dilutes the solution containing the osmotic solute the flows are plotted versus time and the resulting curve extrapolated back to time zero.

Under these conditions, where $\Delta P = 0$, the relationship between volume flow and L_{pD} is reduced to

$$J_{v_o} = L_{pD}\ RT\Delta C_s \qquad (32)$$

Since $RT\Delta C_s$ is easily calculated, and J_{v_o} has been experimentally determined, the equation is easily solved for L_{pD}.

L_p, the hydraulic conductivity of the membrane, is measured by applying a known hydrostatic pressure, ΔP, to one side of the membrane and by following the subsequent volume flow across the membrane. In this procedure there is no solute in the solutions bathing both sides of the membrane, hence, ΔCRT is equal to zero and the relationship becomes

$$J_v = L_p\ \Delta P \qquad (33)$$

Consequently L_p is easily calculated since Δp is known and the resulting J_v is measured.

The L_p of each membrane was determined for every pressure used in experiments as a check on the effect of pressure on the membrane. All membranes used showed constant L_p values within the pressure ranges used in the experiments, which suggests that the applied pressures do not effect the membrane pore size. After both L_{pD} and L_p were determined, σ was calculated from the equation above.

Table IV gives the numerical values of the reflection coefficients determined by the two procedures described on each of the membranes. There is excellent agreement between the two procedures, and as is to be expected, the reflection coefficients increase with increasing size of the solute.

Once the reflection coefficients of a number of solutes have been determined, the effective pore radius of the membrane can be calculated by the method of Goldstein and Solomon (19).

The equation,

$$1-\sigma = \frac{[2(1-a/r)^2 - (1-a/r)^4]\,[1-2.104\ a/r + 2.09\ (a/r)^3 - 0.95\ (a/r)^5]}{[2(1-aw/r)^2 - (1-aw/r)^4]\,[1-2.104\ aw/r + 2.09\ (aw/r)^3 - 0.95]\ (aw/r)^5} \quad (34)$$

Where a = the radius of the solute molecule, aw = the radius of the water molecule, and r = the equivalent pore radius is derived by Goldstein and Solomon from the equation of Renkin (73).

Using this equation it is possible to generate a family of curves $(1-\sigma)$ as a function of the permeant molecular radius. Figure 6 shows the family of curves generated by this equation. Gratitude

Table IV

Solute Reflection Coefficients for Membranes Studied

Solute	Amicon UM-3		S & S B20		G.A. Type B	
	Procedure		Procedure		Procedure	
	1[+]	2[++]	1	2	1	2
Urea	*	*	0.008	*	0.130	*
Mannitol	*	*	0.053	0.058	0.282	0.310
Sucrose	0.02	*	0.092	0.088	0.524	0.509
Raffinose	0.03	0.032	0.103	0.098	0.839	0.808

[+]1. $\sigma = \Delta\Pi/\Delta CRT$

[++]2. $\sigma = \frac{-L_pD}{L_p}$

* Not determined

Figure 6

This figure presents a family of curves generated from equation 34. The abcissa is $1-\sigma$ and the ordinate is the radius of the probe molecules. The number at the top of each line gives the effective pore radius in Å. The data from which these lines were plotted were obtained by Dr. P. F. Curran, Yale University, with a computer program written to solve equation 34.

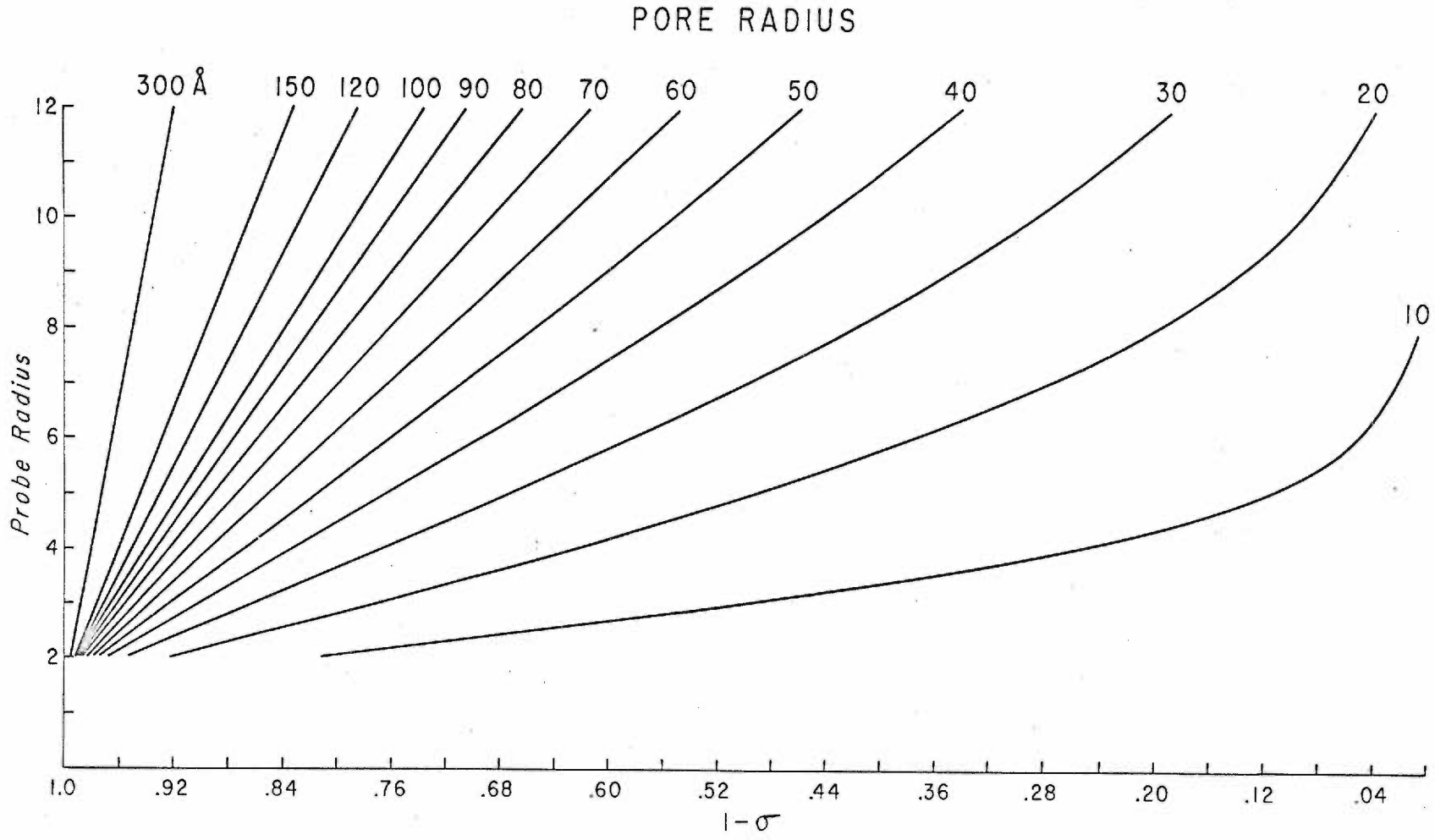
PORE RADIUS
300 Å
150
120
100
90
80
70
60
50
40
30
20
10
Probe Radius
12
10
8
6
4
2
1.0
.92
.84
.76
.68
.60
.52
.44
.36
.28
.20
.12
.04
1 - σ

is expressed to Dr. Peter J. Curran of Yale University School of Medicine for his help in supplying computer calculated values necessary for this plot. Each curve represents a single equivalent pore radius. The equivalent pore radius of the membrane tested is determined by selecting the curve which most closely fits the experimental values of $1-\sigma$. Table I presents the effective pore radius of the membranes used in this study. Line 3 shows the effective radius determined by this method. Line 4 of the same table shows the effective pore radius for the membranes determined by the procedure which compares the diffusive flow of H_2O across a membrane to the viscous flow of H_2O across the same membrane. This method of determining the effective pore radius, which has been used by a number of investigators (27,72,30,74), was initially developed by Pappenheimer et al. (26) and Koefoed-Johnsen and Ussing (20).

The general equation which is used is

$$r = \sqrt{\frac{8\eta L_p D}{P_w}} \tag{35}$$

or

$$r = \sqrt{\frac{8\eta L_p D\bar{V}}{P_w RT}} \tag{36}$$

where η = the viscosity of water, D = the diffusion coefficient of H_2O, R = the ideal gas constant, T = absolute temperature, L_p = hydraulic conductivity coefficient, and P_w = the water permeability

coefficient.

The hydraulic conductivity coefficient, L_p, is determined as described above and P_w, the permeability coefficient for H_2O, is determined by measuring the permeability of THO for the membrane.

A more accurate form of the equation derived by Paganelli and Solomon (27) was used in the calculations of pore radii of the membranes and is shown here in a simplified form as presented by Stein (75).

$$r = -1.5 + \sqrt{4.5 + \left[\left(\frac{L_p}{P_w}\right) - 1\right] \times 14.5} \qquad (37)$$

where aw = 1.5, $\eta = 0.36 \times 10^{-3}$ dyne sec cm^{-1}, $D = 2.59 \times 10^{-5}$ cm^2 sec^{-1}, and r = equivalent radius of pores in $\mathring{A}$.

RESULTS

Studies carried out in our laboratory (8) as well as those of other investigators (9, 55) have shown that hyperosmolarity induced asymmetrical solute fluxes across frog skin are not dependent upon active sodium transport per se. Further, it has been shown that none of the metabolic processes sensitive to DNP, CN^- or ouabain are required for the maintenance of asymmetric solute transport of non-electrolytes under hyperosmotic conditions. These studies, however, do not eliminate the possibility that changes in a "dying" biological system such as the in vitro frog skin preparation may in some unknown way be responsible for the observed phenomena. In other words, the presence of uncontrollable variables inherent in in vitro biological systems makes it difficult to preclude biological participation in the asymmetrical fluxes reported (6,7,55,76). The use of a nonbiological membrane circumvents this problem. If asymmetrical fluxes can be demonstrated in systems containing structurally stable, synthetic membranes, a strong argument may be made for physical rather than for biological forces as the causative agents of the flux asymmetry. To this end we have studied a variety of synthetic membranes with a number of solutes as the hyperosmotic and/or the "tracer" solute.

Initial studies were carried out with the Diaflow UM-3 membrane mounted in the chamber apparatus assembly described earlier

in Figs. 3, 4, and 5. Table V summarizes these studies. Frog Ringer's was used in some of the experiments as bathing solution and tracer fluxes were measured in both directions across the membrane. The UM-3 membrane is anisotropic, and has a shiny and a dull surface. In Table V, S → D refers to the movement of tracer from the solution bathing the shiny surface to the solution bathing the dull surface of the membrane.

As is to be expected, with identical solutions on both sides of the membrane, H_2O, Ringer's and Ringer's-sucrose, flux ratios of inulin-^{14}C were not different from one. Under such conditions, there is no chemical gradient for the tracer solute (i.e., driven) and the flux of the solute is equal in both directions across the membrane. When 0.3 moles L^{-1} of sucrose was included in the Ringer's on one side, (series 3) and a 115 $\mu l\ hr^{-1}\ cm^{-2}$ osmotic flow into this hyperosmotic solution allowed to proceed, the flux in the direction of flow increased while that in the direction opposite to the H_2O flow decreased, resulting in a flux ratio of 0.2.[2] This means that the flux of tracer inulin was greater into the hyperosmotic than out of it and demonstrates the phenomenon of solvent

[2]The flux ratio for synthetic membrane studies is defined as

$$\frac{\text{Flux of the tracer out of the hyperosmotic solution}}{\text{Flux of the tracer into the hyperosmotic solution}}$$

Thus a flux ratio greater or less than one has the same meaning as did ratios for frog skin where the influx represented movement out of the hyperosmotic solution (see equation 1).

Table V

Inulin Flux and Flux Ratios with DiaFlo UM-3 Membrane

Series	No. of Samples	Bathing Solution	Net Volume Flow	Tracer*	$P_I \times 10^3$	Ratio+	Conclusion**
1	20	Ringer's on both	None	D → S	5.9 ± 0.6	1.3	= 1.0
	12	sides	None	S → D	4.5 ± 0.3		
2	16	0.3 M Sucrose-Ringer's	None	D → S	4.0 ± 0.4	1.0	= 1.0
	14	on both sides	None	S → D	4.0 ± 0.5		
3	18	0.3 M Sucrose-Ringer's	Osmotic flow	D → S	1.6 ± 0.2	0.2	< 1.0
	15	on D side	allowed	S → D	8.9 ± 0.5		
4	12	0.3 M Sucrose-Ringer's	Osmotic flow blocked	D → S	23.3 ± 0.8	13.7	> 1.0
	21	on D side	by hydrostatic head	S → D	1.7 ± 0.2		
5++	8	0.3 M Sucrose-Water	Osmotic flow blocked	S → D	23.0 ± 1.3	12.1	> 1.0
	8	on S side	by hydrostatic head	D → S	1.9 ± 0.2		
6++	12	Water on both	None	S → D	3.6 ± 0.2	1.1	= 1.0
	12	sides	None	D → S	3.2 ± 0.3		

*The symbols S → D refer to the movement of tracer inulin from the solution bathing the shiny surface to the solution bathing the dull surface.

+Ratio = $\frac{\text{flux of tracer out of the hyperosmotic solution}}{\text{flux of tracer into the hyperosmotic solution}}$

**As indicated by "t" test of difference from 1.0 with a confidence level of 0.95 or better.

++A similar UM-3 membrane as in 1-4 above but with a different lot number.

drag as described by Anderson and Ussing (3) and by Ginzburg and Katchalsky (30). It would at first glance appear that flux ratios greater than one cannot be produced in the UM-3 membrane.

However, it must be remembered that bulk flow of water through a "wide-pore" membrane, such as the UM-3 (150 Å), will have a much greater effect on solute fluxes than would a comparable flow across a "narrow-pore" membrane such as frog skin or other biological membranes where the pore radius is 10 Å or less (77, 78). This is shown quite clearly by an equation first derived by Kedem and Katchalsky (48) and rewritten here as:

$$J_s = P\Delta C_s + \bar{C}_s (1-\sigma) J_v \qquad (19)$$

Recall that J_s, the net flux of solute s, is due to diffusion described by the first term of the equation, and bulk flow (solvent drag) described by the second term. Notice that as σ, the reflection coefficient of the solute, approaches 1.0 the importance of the bulk flow term decreases. In the case of frog skin, the reflection coefficients of the solutes studied closely approximate 1 and the second term of the equation is very nearly zero. Thus, in frog skin or cellular membranes, bulk flow of solvent will contribute little to the flux of non-electrolytes such as carbohydrates. However, with the wide-pore membranes, such as the UM-3 where the σ for many solutes is small, the contribution of bulk flow to the net solute flux becomes appreciable. As a result the presence of a process such as solute drag may well be masked so that in order to demonstrate it,

the J_v must be held at zero to eliminate the solvent drag effect.

In series 4 of Table V, hydrostatic heads sufficient to decrease net volume flow to essentially zero were imposed on the system described in series 3. Under this condition the flux in the direction out of the hyperosmotic solution increased while that in the opposite direction decreased. These flux values yield a flux ratio of 13.7 which is significantly greater than 1.0. Since in this experiment there was no net volume flow, the only obvious force which could cause a net flux across the membrane is the gradient created by the presence of sucrose on one side of the membrane. Thus, a flux ratio of 13.7 illustrates in a striking way the significance of solute interaction, for, the mere blocking of the solvent flow increased the flux ratio some 68 fold over that where solvent flow was allowed.

The large flux asymmetry reported above is not due to instrumental error or the inability to hold J_v at precisely zero. This is shown by the observation that a net bulk flow of 24 $\mu l\ cm^{-2}\ hr^{-1}$ was required to produce a flux ratio of 12. Since such a large volume flow was required to produce a flux ratio of 12, it is very unlikely that the result shown in series 4 is due to the inability to maintain the volume flow at exactly zero, especially in light of the fact that our measurements of net volume change are equal to or less than 2 $\mu l\ cm^{-2}\ hr^{-1}$, which is some ten times less than that required to produce the flux ratio of 12 under a hydrostatic flow.

It was considered possible that the anisotropic nature of the UM-3 membrane might be responsible for the asymmetric flux cited in series 4 of Table V. To eliminate this possibility, the UM-3 membrane was reversed, the hyperosmotic solution added to the chamber now bathing the shiny side of the membrane, and the osmotic flux blocked as before. This condition (series 5) is identical to that of series 4 but with the membrane turned 180 degrees. It is clear that flux ratios greater than one are obtained and that the fluxes themselves are of the same magnitude as before. It is acknowledged that an additional detail was altered, for, water and water-sucrose solutions were used in series 5 and 6 in place of Ringer's and sucrose-Ringer's solutions. The validity of this approach is attested to by the similarity of the flux values obtained. The data also suggest that an ionic charge is not involved in the phenomenon being described since the presence or absence of electrolytes had no effect on the magnitude of the flux ratios.

Having established the existence of asymmetrical solute transport across synthetic membranes, under conditions similar to those producing flux asymmetry in frog skin, it was decided to investigate further the nature of the process.

If a coupling of flows occurs between the diffusing hyperosmotic agent and the tracer species which has no concentration gradient, one would expect a direct relation between the amount of hyperosmotic agent moving across the membrane and the magnitude of

the flux ratio and net flux of the tracer solute.

Several experiments were carried out to determine the effect of a range of sucrose concentrations on unidirectional inulin fluxes. Fluxes were measured for at least six 5-minute periods into and out of the hyperosmotic solution. In Fig. 7 the arithmetic means of the unidirectional fluxes are plotted against the concentration of the hyperosmotic sucrose solution used. The outflux values are seen to increase linearly with the sucrose concentration while the influxes decrease, also linearly. Notice that the slopes of the fluxes are nearly the same but of opposite sign. This indicates that not only is the outflux increased over some initial value by the action of the hyperosmotic agent but that the influx of solute into the hyperosmotic solution is decreased by approximately the same amount. Hence, the effect of hyperosmolality appears symmetrical with respect to the unidirectional trans-membrane fluxes. The lines of best fit (by regression analysis) for the experimental points intersect the y axis at essentially the same point, suggesting that there will be, as is observed in Fig. 8, no net flux in the absence of the hyperosmotic agent. This y intercept at about 8.0 is a theoretical P value for zero concentration of sucrose. This value of 8.0 is less than the experimentally determined P of 10.9×10^{-3} cm hr^{-1} found when H_2O bathes both sides of the membrane. Presumably, the difference between the values lies in the fact that the viscosity

Figure 7

The effect of increasing concentration of sucrose on one side of the S & S B20 membrane on unidirectional inulin fluxes (P values). The points are average values of at least eight experimental determinations and the bars represent ± 1 SE.

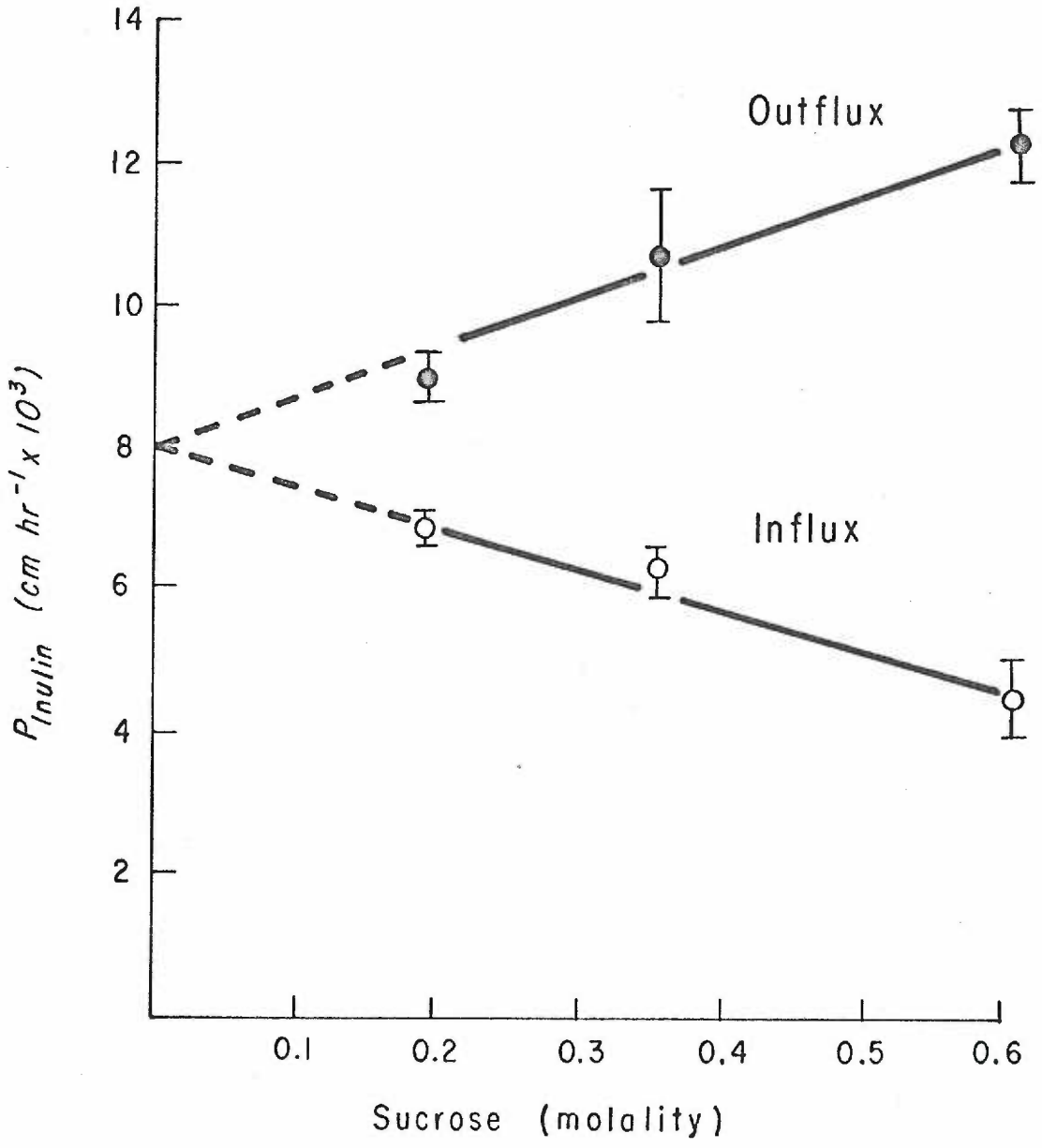
14
12
10
8
6
4
2
Outflux
Influx
P_{Inulin} (cm hr^{-1} x 10^3)
0.1
0.2
0.3
0.4
0.5
0.6
Sucrose (molality)

Figure 8

The relationship between the inulin flux ratio and the hyperosmotic sucrose concentration. The flux ratios represented by each point are calculated from the mean values of at least eight experimental determinations of unidirectional inulin fluxes across the S & S B20 membrane.

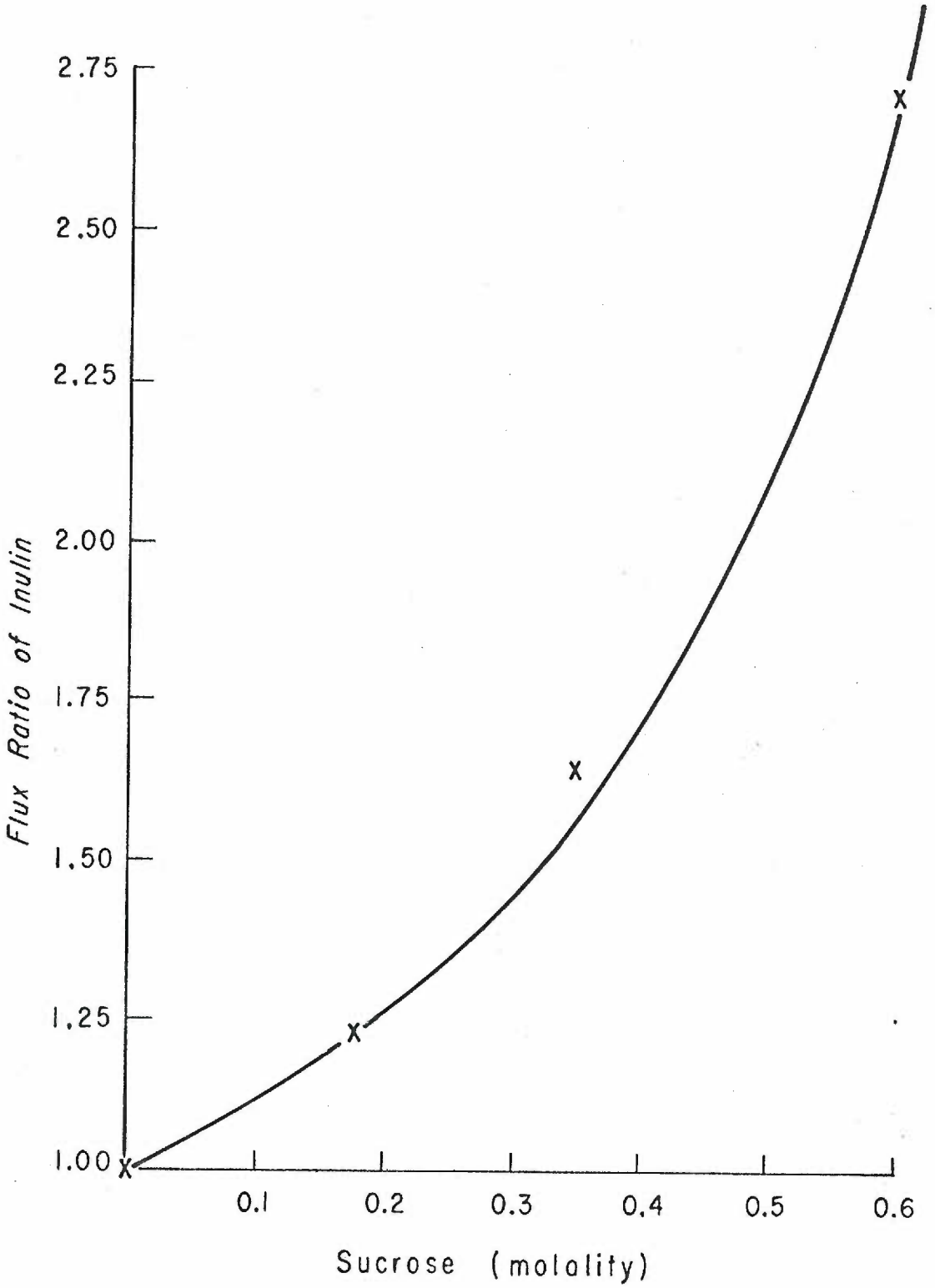
2.75
2.50
2.25
2.00
1.75
1.50
1.25
1.00
Flux Ratio of Inulin
0.1
0.2
0.3
0.4
0.5
0.6
Sucrose (molality)

effects of the hypertonic solutions are not corrected for in extrapolating to zero sucrose concentration. As shown in Table V, P values in 0.3 M sucrose solutions are also about 20 percent less than those determined with Ringer's bathing both sides of the membrane.

Figure 9 presents the results of two parallel series of experiments. In one, the sucrose ^{14}C tracer flux was measured at various concentrations of sucrose under the same conditions as those in series 5 of Table V. In the second series of experiments the inulin-^{14}C flux was measured with various concentrations of sucrose. The net fluxes of sucrose and inulin were then calculated and plotted with respect to the concentration of the so-called hyperosmotic agent.

The plotted points represent the arithmetic means of at least eight experimental periods for the flux of each tracer and correspond to sucrose concentrations of 0, 0.175, 0.35 and 0.6 moles per kg of H_2O from the lowest to the highest net fluxes respectively. Clearly the inulin outflux is a linear function of the concomitant sucrose outflux. This observation indeed suggests a coupling of the sucrose and inulin flows and is in agreement with the observations of Biber and Curran (55) for toad skin with mannitol as the driven solute and urea as the hyperosmotic agent.

The relationship between the concentration of the sucrose and the flux ratio of inulin is summarized in Fig. 8. As is to be expected from Fig. 7, the flux ratio is not a simple, linear function

Figure 9

The relationship between net sucrose outflux and net inulin outflux on the S & S B20 membrane. Each point represents the mean of at least eight determinations. The sucrose concentration on the acceptor side was in each case 0.001 M. At X_1, X_2, X_3, and X_4 the sucrose concentration on the donor side was 0.001, 0.175, 0.350, and 0.600 m respectively.

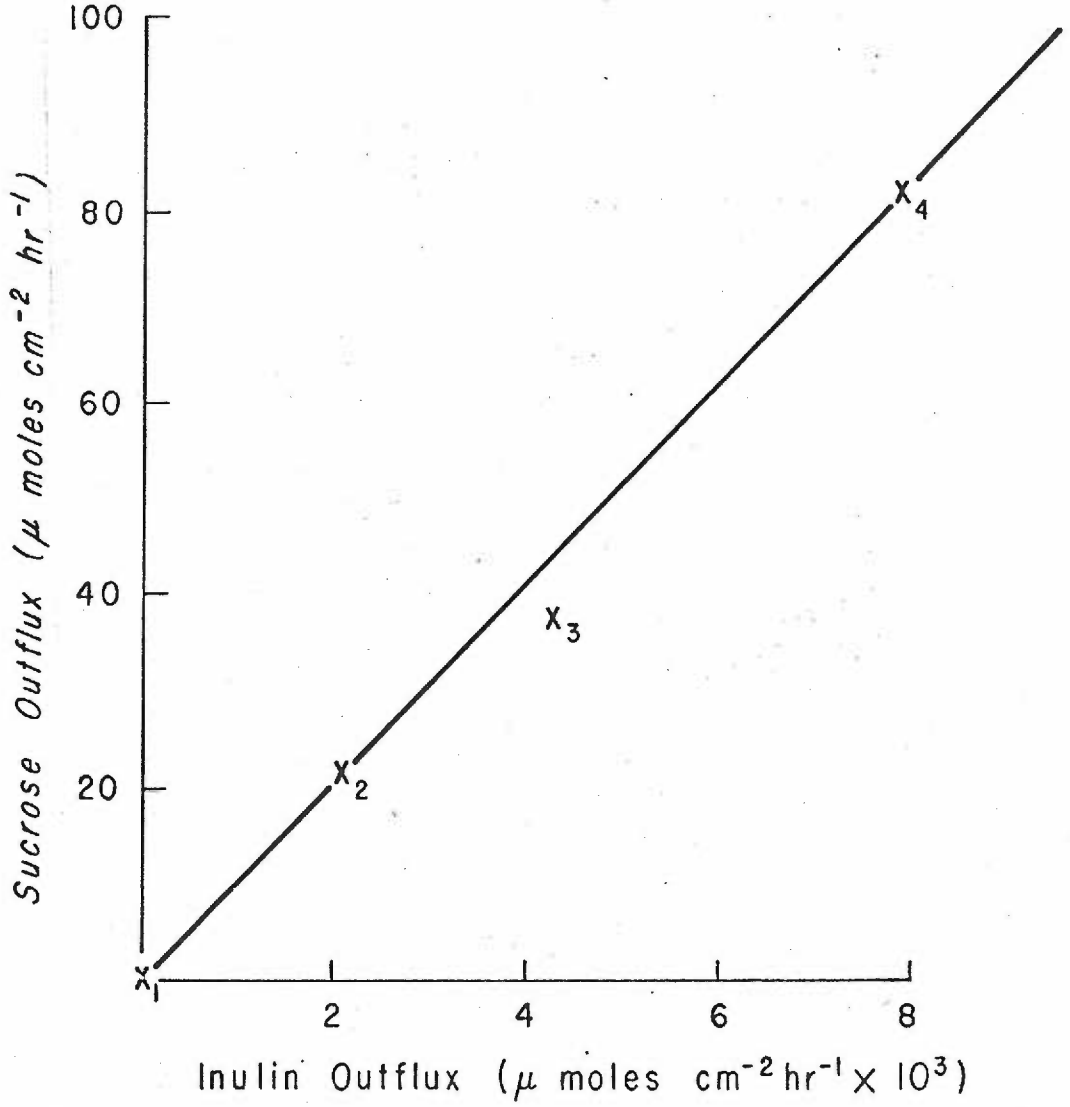
100
80
60
40
20
Sucrose Outflux (μ moles cm⁻² hr⁻¹)
X1
X2
X3
X4
2
4
6
8
Inulin Outflux (μ moles cm⁻² hr⁻¹ X 10³)

of sucrose concentration. Since the flux ratio is the ratio of the unidirectional fluxes the equation for this curve can be written as:

$$y = \frac{7.05x + 8.03}{5.78x + 8.10} \qquad (38)$$

Where y = inulin flux ratio, x = hyperosmotic sucrose concentration and 7.05 and 5.78 are the slopes of the lines generated by the outflux and influx values of Fig. 7; 8.03 and 8.10 are the extrapolated y intercepts of these same two lines from Fig. 6.

If there is indeed coupling between the flows of the diffusible solutes, one might expect the effectiveness of a solute to couple and thus create flux ratios greater than one, to vary both with its permeability and/or its molecular size.

Consequently, it was decided to investigate solutes of different sizes with respect to their action as both hyperosmotic and tracer solutes. The studies were carried out on the S & S B20 membrane. The B20 membrane was selected for this rather extensive study because of its small pore radius (see Table I), its reported uniform structure (58) and, as found by experience, its relative stability.

The following section describes the results of the studies carried out with the S & S B20 membrane.

Figure 10 presents the P values of the tracer species when H_2O bathes both sides of the membrane. The reported values

Figure 10

P values and flux ratios of solutes with 1 mM aqueous solutions of the tracer species bathing both sides of the S & S B20 membrane. W = THO (tritiated water), M = mannitol, S = sucrose, R = raffinose, I = inulin, D_I = 16,000-19,000 MW dextran, and D_{II} = 60,000-90,000 MW dextran. Each bar represents the mean of at least eight experimental periods.

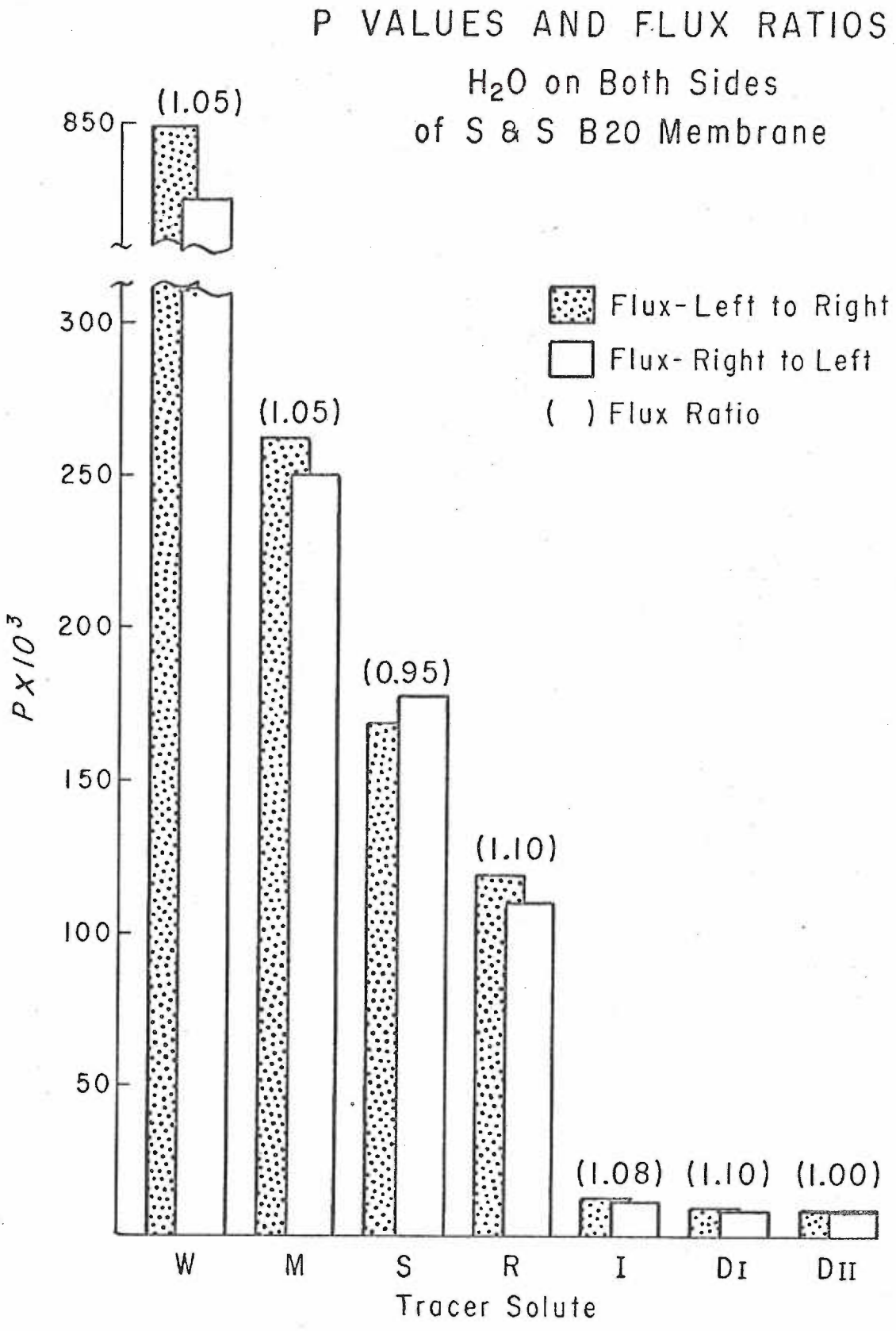
P VALUES AND FLUX RATIOS
H2O on Both Sides
of S & S B20 Membrane
Flux-Left to Right
Flux-Right to Left
( ) Flux Ratio
P X 10³
850
300
250
200
150
100
50
(1.05)
(1.05)
(0.95)
(1.10)
(1.08)
(1.10)
(1.00)
W
M
S
R
I
DI
DII
Tracer Solute

are the arithmetic means of eight or more sample periods. It is evident from this histogram that the permeabilities of the solutes decrease with increasing molecular size, just as diffusion coefficients decrease with increasing molecular size (79). Also, it is likely that in a membrane having pores with a range of sizes, the larger molecular species will have fewer pores through which they can penetrate.

A second conclusion which may be arrived at from the data summarized in Fig. 10 is that the flux ratios of none of the tracer solutes are different from 1.0 as determined by "t" test with a confidence level of 0.95 or better. These ratios indicate that in spite of possible structural and mechanical asymmetry of the system, symmetric fluxes are indeed obtained. Figure 11 relates the permeability coefficients for six of the seven tracer solutes reported in Fig. 10 with 0.35 m sucrose bathing both sides of the B20 membrane. The values represent the arithmetic means of eight or more observations. It is evident that the relative order of magnitude of P values seen in the system with H_2O bathing both sides is retained. In other words, $P_{man.} > P_{suc.} > P_{raf.} > P_I > P_{dex.}$

It is also of interest that the absolute magnitudes of all the tracer permeabilities except those for tritiated H_2O have decreased. This is quite probably due to the decrease in diffusion coefficients caused by the more viscous hyperosmotic solution (79). Although the P values decreased somewhat in the more concentrated

Figure 11

P values and flux ratios of the tracer solutes with solutions, which are 1 mM in the tracer solute and 0.35 m in sucrose, bathing both sides of the S & S B20 membrane. W = tritiated water, M = mannitol, S = sucrose, R = raffinose, I = inulin, D_I = 16,000-19,000 MW dextran, D_{II} = 60,000-90,000 MW dextran. Each bar represents at least eight experimental determinations of the P value.

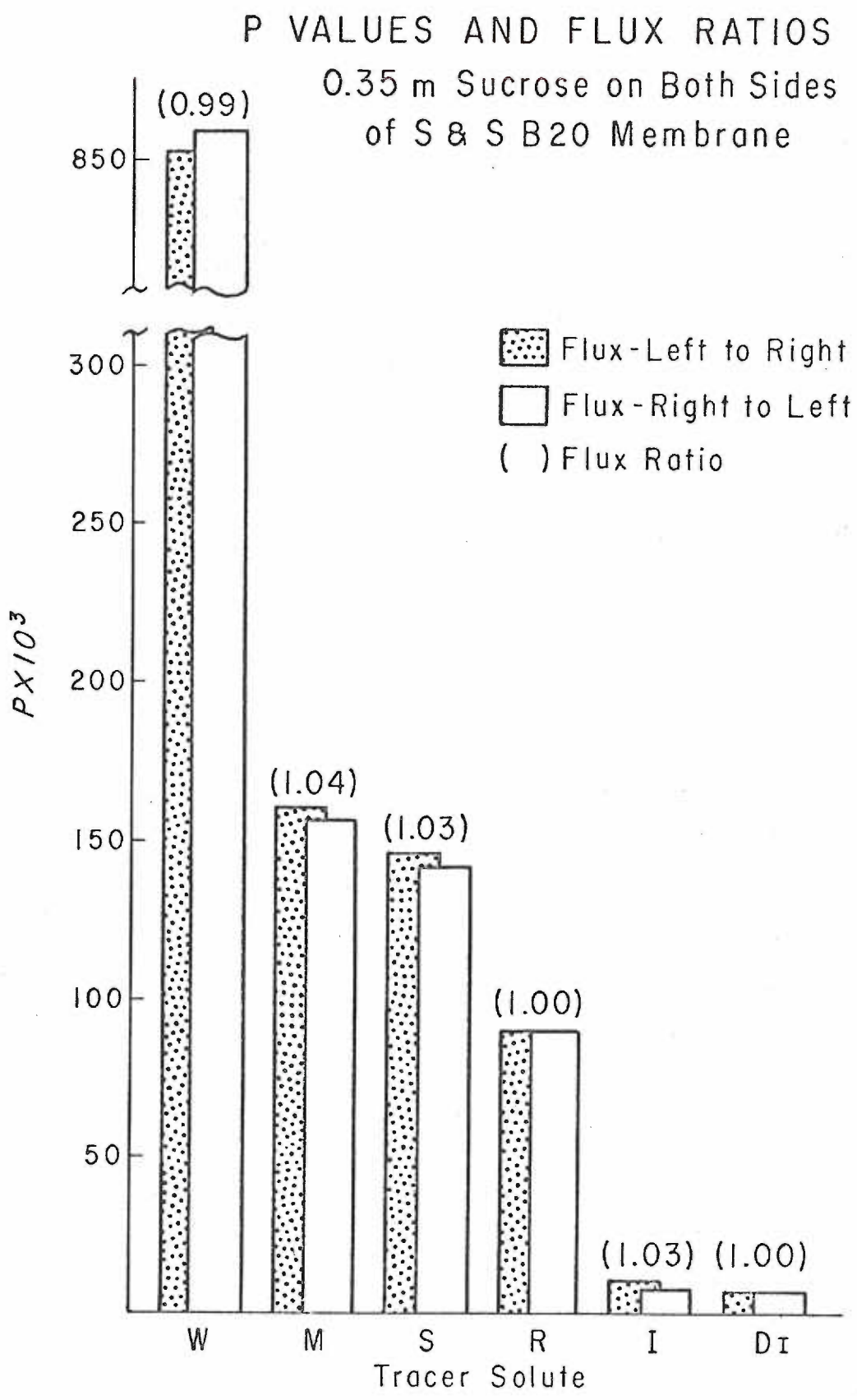
P VALUES AND FLUX RATIOS
0.35 m Sucrose on Both Sides
of S & S B20 Membrane
(0.99)
850
300
250
200
150
100
50
PX10³
Flux-Left to Right
Flux-Right to Left
( ) Flux Ratio
(1.04)
(1.03)
(1.00)
(1.03)
(1.00)
W
M
S
R
I
DI
Tracer Solute

solutions, it is important that the flux ratios were again not different from 1.0, as determined by the "t" test at a confidence level of 0.95 or better. Although only the P values obtained for the 0.35 m sucrose system are presented in Fig. 11, hyperosmotic solutions of mannitol, raffinose and dextran show similar effects.

In Figs. 12, 13 and 14, 0.35 m solutions of the hyperosmotic agent were placed on one side of the membrane and radioactively labeled tracer solute was added to an appropriate side. Both bathing solutions were made 1 mM with the tracer solute, so that a concentration gradient for the tracer species was avoided. Hydrostatic pressure was applied to the chamber containing the hyperosmotic solution until the net volume flow across the membrane was less than $\pm$ 2 $\mu l\ cm^{-2}\ hr^{-1}$. Tracer fluxes across the membrane were then measured into and out of the hyperosmotic solution. The basic experiment is analogous to series 5 of Table V.

Figure 15 presents the same data obtained with 0.008 m dextran with an average molecular weight 16,900 as the hyperosmotic solution. Several quite interesting findings are clearly shown in these figures.

First notice that with any hyperosmotic agent the relative order of magnitude of the P values for mannitol, sucrose, raffinose and inulin seen in Figs. 10 and 11 is preserved. In no case does an influx or outflux of any one of these four tracer solutes increase to a value larger than that of a smaller solute. Hence it appears

Figure 12

P values and flux ratios for tracer solutes with 0.35 M mannitol on one side of the membrane and with osmotic flow blocked by hydrostatic pressure, i.e., $J_v = 0$. Flux ratios are calculated from the P values for outfluxes and influxes. The P values (as cm hr^{-1}) for the unidirectional fluxes reported are the means of at least eight experimental periods. The standard error of the means are seen below.

	SE of mean	
	Outflux	Influx
M = mannitol	± 6.8	± 9.5
S = sucrose	± 4.9	± 4.9
R = raffinose	± 2.2	± 1.1
I = inulin	± 0.4	± 0.4
D_I = 16,000-19,000 MW dextran	± 0.4	± 0.4
D_{II} = 60,000-90,000 MW dextran	± 0.6	± 0.4

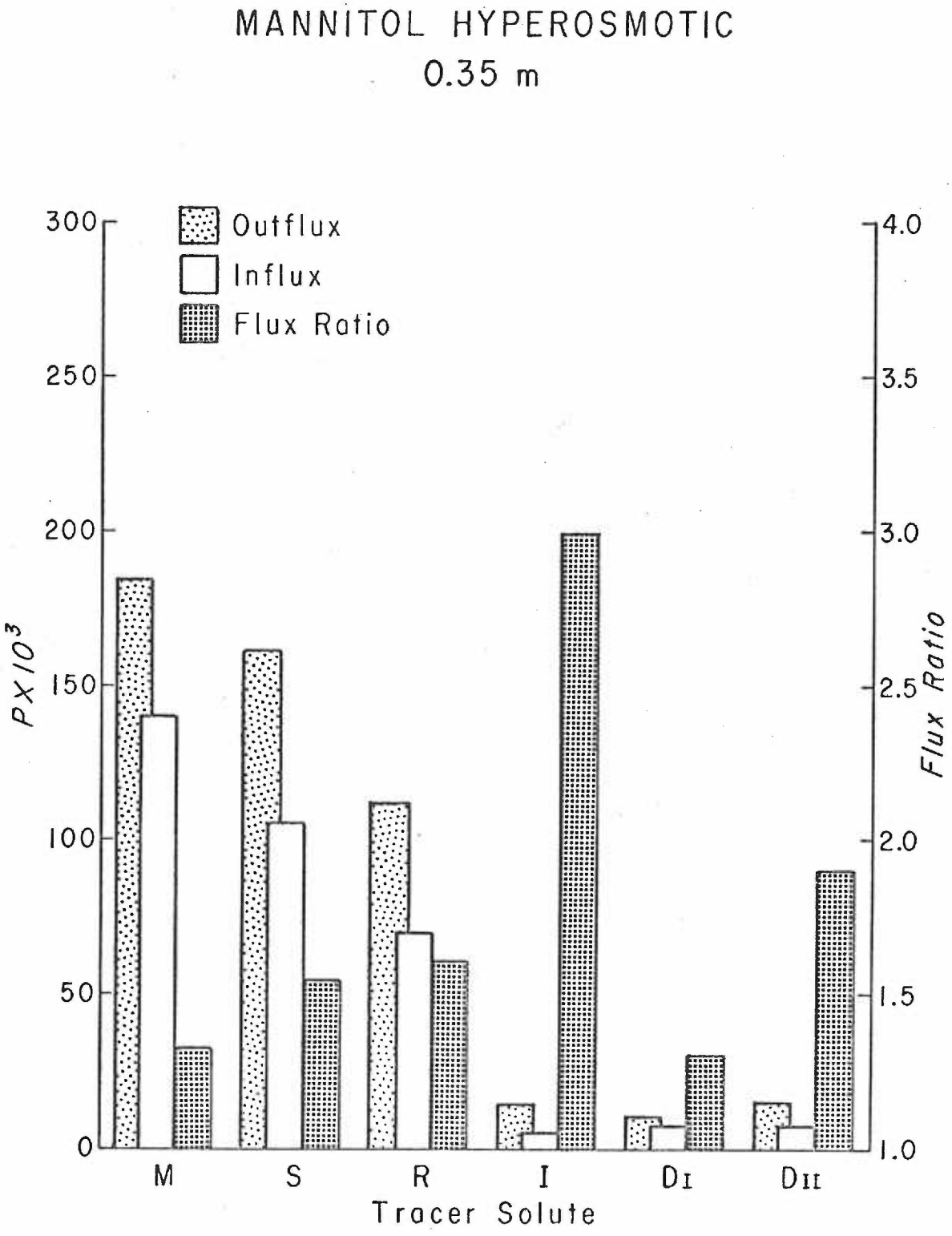
MANNITOL HYPEROSMOTIC
0.35 m
Outflux
Influx
Flux Ratio
300
250
200
150
100
50
0
PX10³
4.0
3.5
3.0
2.5
2.0
1.5
1.0
Flux Ratio
M
S
R
I
DI
DII
Tracer Solute

Figure 13

P values and flux ratios for tracer solutes with 0.35 m sucrose on one side of the membrane and with osmotic flow blocked by hydrostatic pressure, i.e., $J_v = 0$. Flux ratios are calculated from the P values for outfluxes and influxes. The P values (as cm hr^{-1}) for the unidirectional fluxes reported are the means of at least eight experimental periods. The standard error of the means are seen below.

	SE of mean	
	Outflux	Influx
M = mannitol	± 8.9	± 5.0
S = sucrose	± 5.9	± 1.6
R = raffinose	± 2.9	± 1.8
I = inulin	± 0.5	± 0.13
D_I = 16,000-19,000 MW dextran	± 0.2	± 0.4
D_{II} = 60,000-90,000 MW dextran	± 0.9	± 0.2

SUCROSE HYPEROSMOTIC
0.35 m

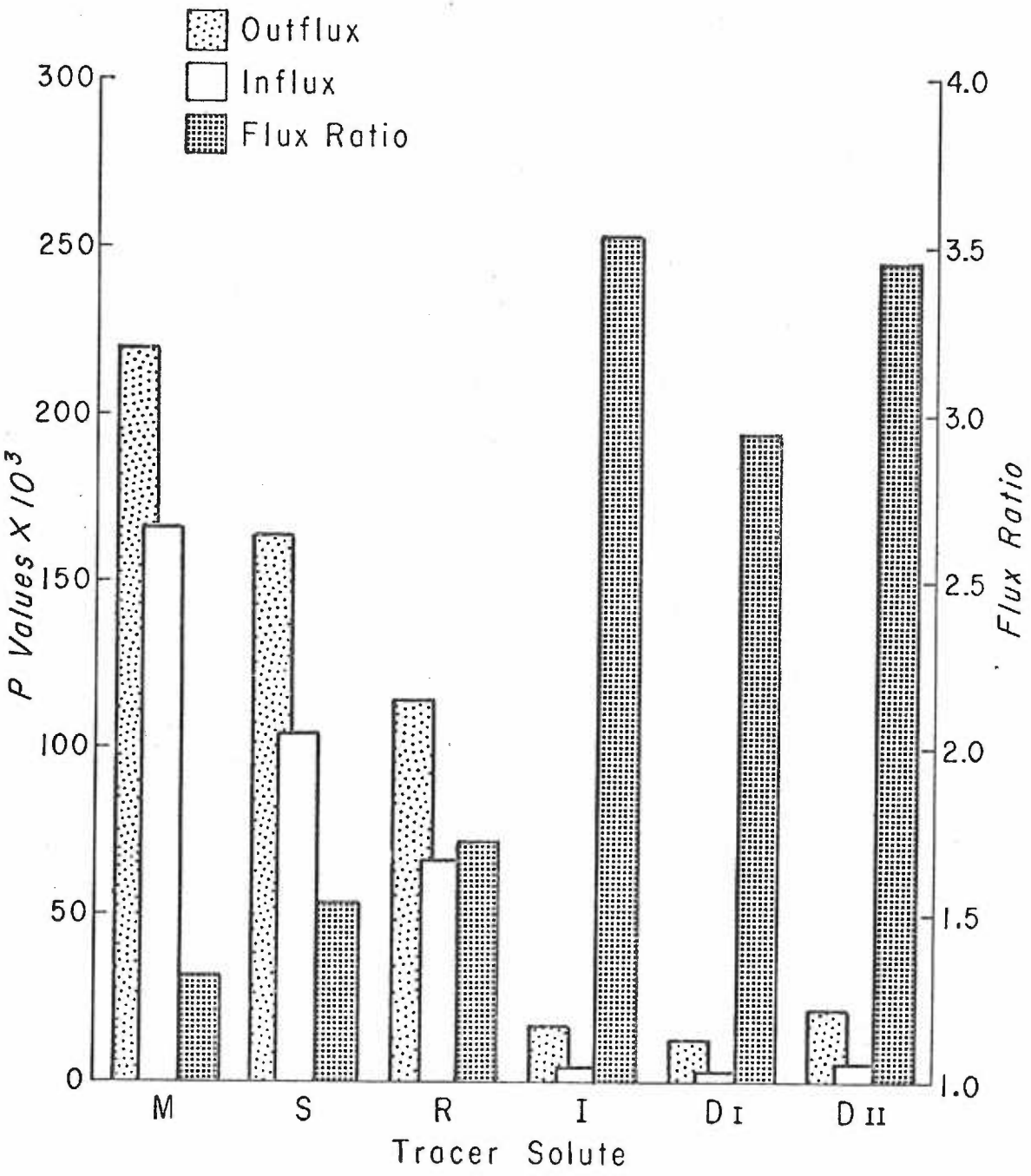

Figure 14

P values and flux ratios for tracer solutes with 0.35 M raffinose on one side of the membrane and with osmotic flow blocked by hydrostatic pressure, i.e., $J_v = 0$. Flux ratios are calculated from the P values for outfluxes and influxes. The P values (as cm hr^{-1}) for the unidirectional fluxes reported are the means of at least eight experimental periods. The standard error of the means are seen below.

	SE of mean	
	Outflux	Influx
M = mannitol	± 5.7	± 4.3
S = sucrose	± 3.2	± 1.5
R = raffinose	± 4.2	± 1.3
I = inulin	± 0.6	± 0.3
D_I = 16,000-19,000 MW dextran	± 1.3	± 0.2
D_{II} = 60,000-90,000 MW dextran	± 0.6	± 0.4

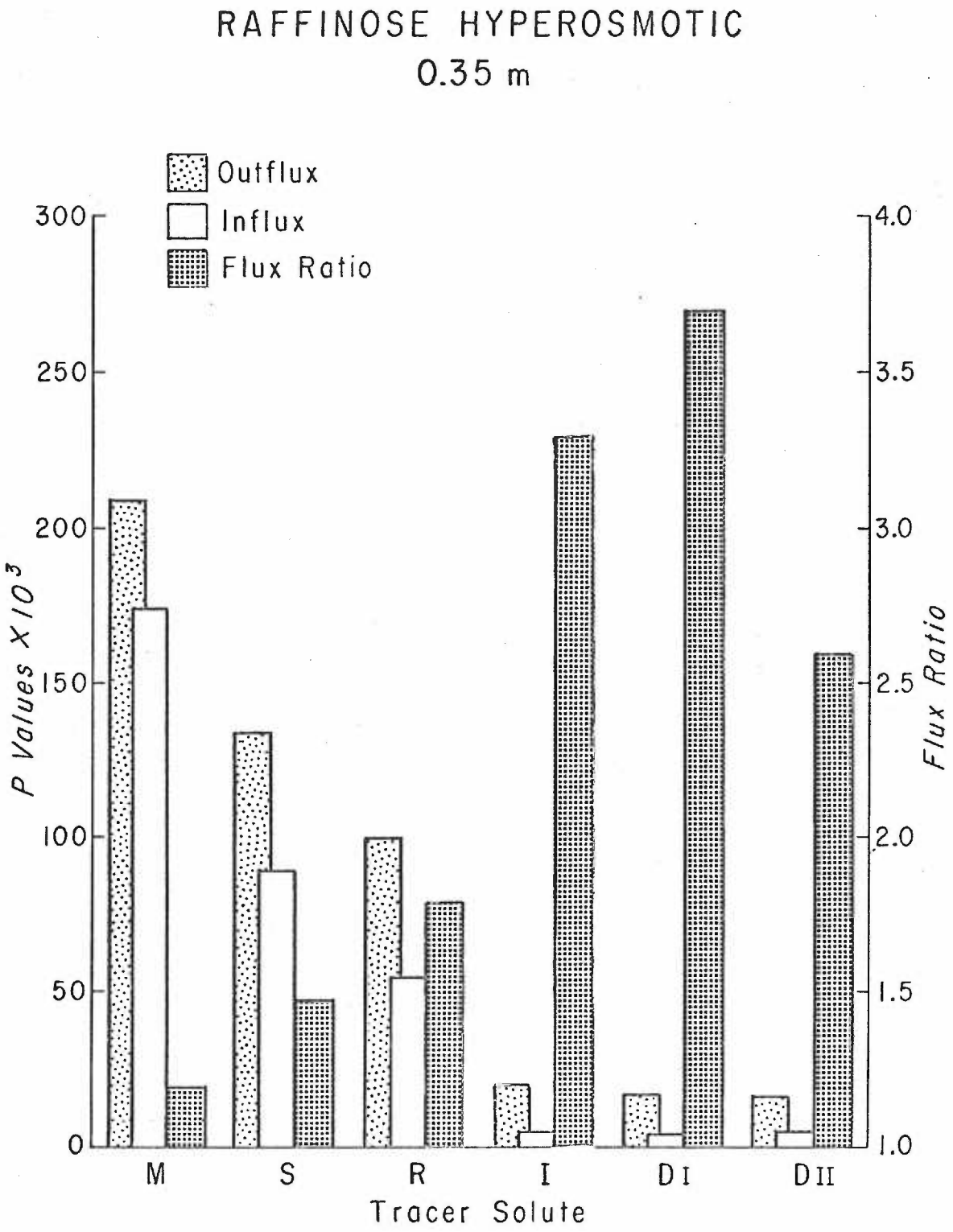
RAFFINOSE HYPEROSMOTIC
0.35 m
Outflux
Influx
Flux Ratio
300
250
200
150
100
50
0
4.0
3.5
3.0
2.5
2.0
1.5
1.0
P Values X 10³
Flux Ratio
M
S
R
I
DI
DII
Tracer Solute

Figure 15

P values and flux ratios for tracer solutes with 0.008 M ∿16,500 MW dextran on one side of the membrane and with osmotic flow blocked by hydrostatic pressure, i.e., $J_v = 0$. Flux ratios are calculated from the P values for outfluxes and influxes. The P values (as cm hr^{-1}) for the unidirectional fluxes reported are the means of at least eight experimental periods. The standard error of the means are seen below.

	SE of mean	
	Outflux	Influx
M = mannitol	± 5.5	± 5.1
S = sucrose	± 4.7	± 3.5
R = raffinose	± 2.3	± 1.4
I = inulin	± 0.7	± 0.6
D_I = 16,000-19,000 MW dextran	± 1.2	± 1.1
D_{II} = 60,000-90,000 MW dextran	± 0.3	± 0.7

DEXTRAN HYPEROSMOTIC
0.008 m

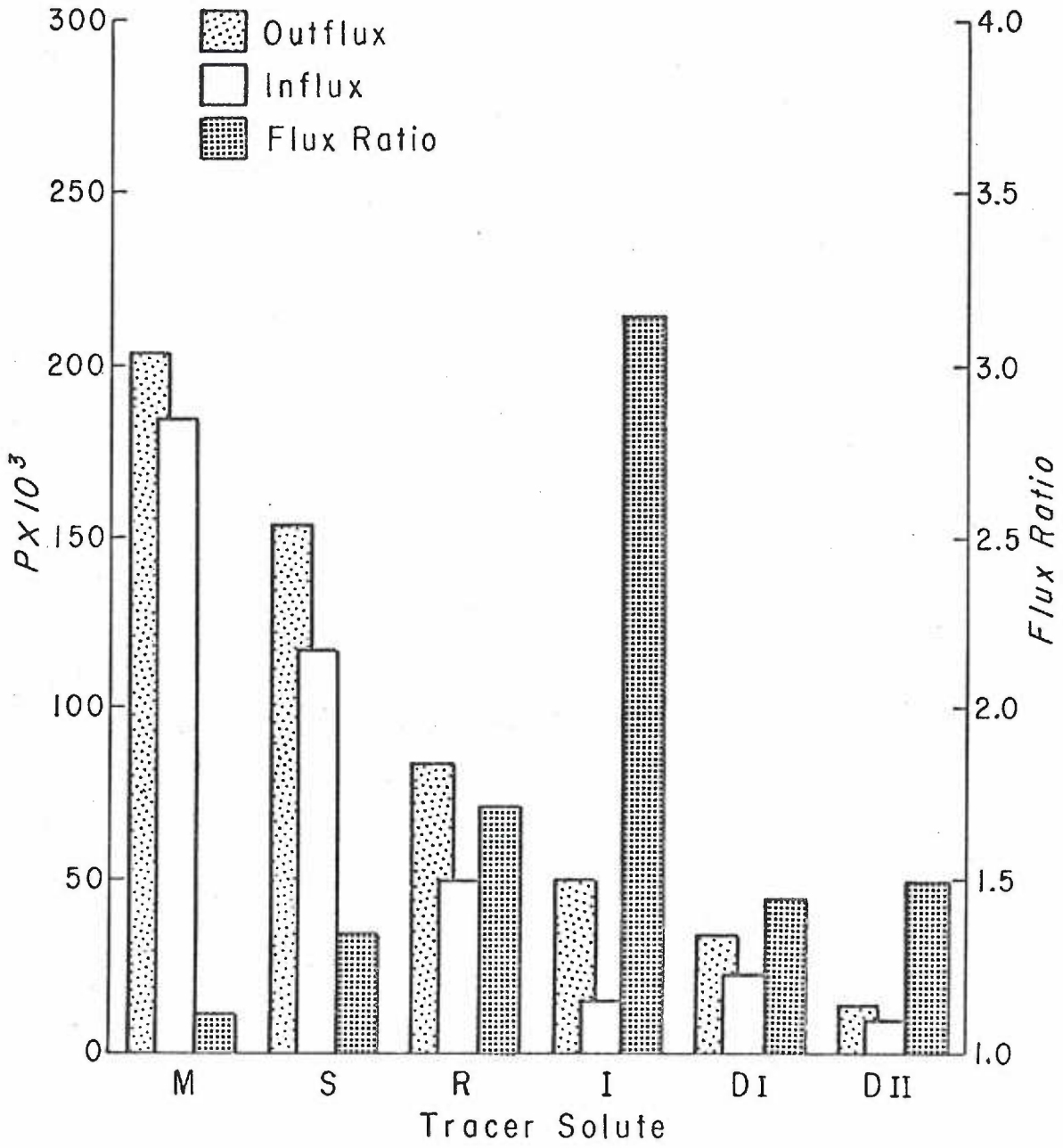

that whatever force is acting on the tracer solutes is acting universally on all of these solutes. In other words, molecularly specific interaction within this group of carbohydrates does not occur between the hyperosmotically induced force and a particular solute.

However, the relative permeabilities of the two dextran tracers appear to be reversed by the hyperosmotic mannitol and sucrose. That is, the larger dextran becomes more permeable than the smaller dextran fraction under the conditions of the smaller hyperosmotic solutes such as mannitol or sucrose. This observation is not easily explained if one assumes the dextran molecules to be spherical in shape. A possible explanation of this observation will be presented later in this thesis.

The second interesting observation from the data presented in Figs. 12 through 15 is that with the 0.35 M solutions of hypertonic solutes the P values of the tracer mannitol, sucrose and raffinose never exceed those observed when H_2O bathes both membrane surfaces. It appears that in the case of the larger tracer solutes, the force created by the hyperosmotic agent is large enough to overcome the decrease in permeability resulting from the increased viscosity, whereas the smaller tracer solutes are not as greatly influenced by this force. This suggests that the molecular size of the tracer solute may be important in determining the magnitude of the interaction between solute flows. This possibility is further

supported by the fact that the increase in influx values for inulin and the two dextran species become greater as the size of the hyperosmotic agent increases. Further considerations of these observations are discussed at a later point.

The most obvious fact which can be seen from Figs. 12 through 15 is that the flux ratios of all tracer solutes in the presence of any hyperosmotic agent are all greater than 1.0. Hence, it is evident that flux asymmetry created by the unequal distribution of a solute across a membrane is a general property of the series of solutes investigated rather than a specific effect of a particular solute such as sucrose.

Perhaps the most interesting finding of all in Figs. 12, 13, 14 and 15 is that the flux ratios created by a given hyperosmotic solute increase with the molecular size of the tracer specie. That is, the flux ratio observed with sucrose as a tracer solute is greater than the flux ratio observed with mannitol as the tracer, but smaller than the flux ratio of raffinose as the tracer solute, given any hyperosmotic agent. This is good evidence that the mechanism by which flux asymmetry is created is directly related to the size of at least the tracer solute. Notice that no matter which hyperosmotic agent is used, only moderate increases in the flux ratio are seen from mannitol to sucrose and from sucrose to raffinose as tracer solutes. These increases correspond to increases in the molecular radius of the solutes from about 4.4 to 5.3 to 6.1 Å (see Table II). The increase in the flux ratios from raffinose to inulin

as a tracer species corresponds to about a three-fold increase in flux asymmetry no matter which hyperosmotic agent is used. This large increase in flux asymmetry is coincident with an increase in the molecular radius from 6.1 to ∿15 Å, the largest increase in molecular size between any two consecutive solutes in the series. Consequently, this observation reinforces the initial indication that the mechanism responsible for flux asymmetry is at least dependent on the molecular size of the "tracer" solute. The flux ratios of the two dextran species do not follow the increases in flux ratio seen with the increasing size of the smaller tracers, although in every case, their flux ratios are significantly greater than 1.0. Since the three dimensional structure of the dextran preparation is so poorly understood and the mechanism of its transport under the above conditions completely unknown, the contribution of these studies to the understanding of the phenomenon being investigated is limited. It is, therefore, important that the observations of more completely characterized solutes play the major role in the interpretation of the observed phenomenon.

Table VI is a compendium of the flux ratios obtained in the experiments described by Figs. 11 through 14. In it we see the flux ratios of the tracer specie at the bottom of each vertical column with the hyperosmotic agent seen at the left of each horizontal line. As has just been discussed, the flux ratio resulting from any hyperosmotic agent increases with the molecular size of the tracer

COMPENDIUM OF FLUX RATIOS - S&S B20

Hyperosmotic Agent	Mannitol	Sucrose	Raffinose	Inulin	Dextran I	Dextran II
None (H_2O)	1.05	0.95	1.10	1.08	1.10	1.00
Mannitol	1.32	1.57	1.61	2.98	1.30	1.88
Sucrose	1.32	1.54	1.72	3.54	2.96	3.47
Raffinose	1.20	1.48	1.80	3.29	3.70	2.60

Tracer Solute

solute from mannitol to inulin. Notice, however, that there is no corresponding increase in flux asymmetry with increases in the size of the hyperosmotic agent given a particular tracer solute. The observation that flux asymmetry increases with increasing molecular size of the tracer solute leads one to consider the effect of increasing the size of the hyperosmotic agent on the magnitude of interaction. The net flux of a solute created by several hyperosmotic agents presented in the vertical columns of Table VI is not a direct measure of the amount of interaction between the solutes because, although a large hyperosmotic agent may interact to a greater extent with a given tracer solute, the flux asymmetry which it can create is limited by its decreased permeability. In other words, although the large hyperosmotic solute will be more effective at "sweeping out a pore" once it is inside the pore, fewer of the large solute molecules will be able to move through the pore in the same interval. Consequently, the flux ratio for a given tracer may not increase with increasing molecular size of the hyperosmotic agent.

At this point it becomes profitable to apply some of the equations derived from irreversible thermodynamics.

Recall that under the condition of zero volume flow the net flux of a solute across a membrane in the presence of a second solute may be described by equation

$$J_1 = P_{11}\Delta C + P_{12}\Delta C_2 \qquad (25)$$

As is the case in the experimental procedure described earlier, when there is no concentration gradient for solute 1 (the tracer solute) the flux equation reduces to

$$J_1 = P_{12}\Delta C_2 \qquad \text{when } J_v = 0 \text{ and } \Delta C_1 = 0 \qquad (27)$$

In this case the net flux of solute 1 is dependent solely upon the cross-term permeability coefficient P_{12}. Rearranging the equation we obtain an expression for P_{12}, which quantitates the effect of the concentration of solute 2 on the flux of solute 1, the tracer species.

$$P_{12} = \frac{J_1}{\Delta C_2} \qquad J_v \text{ and } \Delta C_1 = 0 \qquad (28)$$

In other words P_{12} is a measure of the flux of solute 1 produced by a unit concentration of solute 2.

Since we are interested in the coupling of flows between solute 1 and solute 2, the ratio of the cross coefficient, P_{12}, to the straight coefficient of the diffusing hyperosmotic agent, P_{22}, results in a value which reflects the effectiveness of a diffusing hyperosmotic agent at creating asymmetrical solute flow. Hence we may write:

$$\text{The effectiveness of a diffusing hyperosmotic at creating asymmetric flux} = \frac{P_{12}}{P_{22}} \qquad (29)$$

This ratio indicates the amount of asymmetric flux produced

per unit flux of the hyperosmotic agent, hence is a good measure of the coupling between two solute fluxes. In these calculations, the net flux of each tracer solute, J_1, is obtained by subtracting the tracer flux into the hyperosmotic solution from the tracer flux out of the hyperosmotic solution. The P_{22} value used in the calculation of P_{12}/P_{22} is the tracer permeability coefficient of solute 2 out of a 0.35 m solution of itself under the hyperosmotic-hydrostatic pressure conditions. The ΔC_2 is 350 millimolal except for dextran which is ~8 millimolal. The P_{22} for the hyperosmotic dextran specie (average = 19,900) is taken to be that of the smaller of the two tracer dextrans. Table VII presents the calculated values of P_{12} and P_{12}/P_{22} for each tracer paired with each of the four hyperosmotic agents used in the experiments described in Figs. 12 through 15.

Notice that <u>for any tracer solute</u> the ratio P_{12}/P_{22} increases with increasing size of the hyperosmotic agent. This shows that the asymmetric force created by the diffusible hyperosmotic is proportional to the size of the hyperosmotic agent as well as the size of the tracer species. Also notice that the largest increase in P_{12}/P_{22} comes between raffinose and dextran, the largest increase in molecular size between any two of the hyperosmotic agents. This further confirms earlier evidence that the degree of asymmetric force is proportional to the size of the hyperosmotic agent.

It was not possible to examine the effect of a hyperosmotic

Table VII

P_{12} and P_{12}/P_{22} Values for the SS B20 Membrane

Solutes		Cross Coefficient	Interaction Ratio
Tracer 1	Hyperosmotic 2	$P_{12} \times 10^3$ cm hr^{-1}	$P_{12}/P_{22} \times 10^4$
Mannitol	M	0.127	6.8
	S	0.151	9.2
	R	0.101	10.1
	D*	2.59	749.7
Sucrose	M	0.174	9.4
	S	0.170	10.3
	R	0.124	12.5
	D*	4.66	135.1
Raffinose	M	0.123	6.6
	S	0.137	8.3
	R	0.124	12.5
	D*	4.85	140.6
Inulin	M	0.029	1.5
	S	0.036	2.1
	R	0.042	4.2
	D*	4.64	134.5
Dextran I	M	0.007	0.3
	S	0.026	1.5
	R	0.038	3.8
	D*	1.44	417.3
Dextran II	M	0.021	1.1
	S	0.045	2.7
	R	0.032	3.2
	D*	0.613	177.6

*D = ~16,500 MW Dextran at 0.008 m

agent larger than the effective pore of this membrane due to the limited solubility of large macromolecules.

Having accumulated evidence that the magnitude of flux asymmetry is proportional to the sizes of both the hyperosmotic and tracer solutes, it was considered necessary to determine the role of another variable, the pore size of the membrane, in the process producing flux asymmetry. For this purpose, two additional membranes were selected for study. The first of these was another Diaflow UM-3 membrane which had a pore radius of about 350 Å, compared to the 75 Å pore radius of the S & S B20 membrane and the General Atomic Type "B" desalinization membrane with an effective pore radius of ∿25 Å.

As can be seen in Table VIII these membranes also show increasing flux ratios with increasing size of the tracer solute given a particular hyperosmotic agent, see lines 1, 2, 3 and 10, 11, 12 for the UM-3 and the G.A. "B" membranes respectively. Here, it is seen that with mannitol as the hyperosmotic agent, flux ratios increase from mannitol to sucrose to raffinose for all three membranes supporting the previous observations shown in Figs. 12 through 15.

An observation of more than passing interest is seen in Table IX, where representative flux ratios for the three membranes are compared. Notice that as the effective pore radius of the membranes becomes smaller the observed flux ratio for a particular

Table VIII

P Values and Flux Ratios for UM-3 and G.A. Type B Membranes

Membrane	Hyperosmotic Solute	Tracer Solute	Outflux $Px10^3 \pm 1$ SE	Influx $Px10^3 \pm 1$ SE	Flux Ratio Outflux/Influx
UM-3 #2	Mannitol	M	30.6 ± 1.7	29.5 ± 1.6	1.04
		S	22.1 ± 0.8	17.4 ± 0.5	1.27
		R	20.6 ± 1.2	15.3 ± 1.0	1.34
	Sucrose	M	-	-	-
		S	21.3 ± 1.1	18.4 ± 0.6	1.15
		R	19.6 ± 0.8	16.0 ± 1.2	1.22
	Raffinose	M	27.8 ± 1.6	24.2 ± 1.4	1.15
		S	20.1 ± 1.1	17.3 ± 0.8	1.16
		R	21.6 ± 1.3	13.9 ± 0.8	1.56
G.A. "B"	Mannitol	M	222.9 ± 5.5	139.7 ± 5.8	1.59
		S	83.9 ± 3.6	29.0 ± 1.2	2.89
		R	70.4 ± 1.8	27.2 ± 0.6	2.60
	Sucrose	M	176.5 ± 5.0	121.4 ± 5.8	1.45
		S	89.6 ± 3.1	25.8 ± 1.3	3.48
		R	80.9 ± 2.2	22.4 ± 0.9	3.60
	Raffinose	M	171.8 ± 7.7	132.0 ± 5.2	1.30
		S	96.9 ± 2.2	34.0 ± 1.4	2.85
		R	94.1 ± 3.1	29.2 ± 1.0	3.22

Table IX

Comparison of Flux Ratios

for Three Membranes Differing in Effective Pore Radius

Solutes		Flux Ratios		
Hyperosmotic	Tracer	UM-3	S&S B20	GA "B"
Mannitol	M	1.04	1.32	1.59
	S	1.27	1.57	2.89
	R	1.34	1.61	2.60
Sucrose	M	-	1.32	1.45
	S	1.15	1.54	3.48
	R	1.22	1.72	3.60
Raffinose	M	1.15	1.20	1.30
	S	1.16	1.48	2.85
	R	1.56	1.80	3.22

tracer and hyperosmotic pair generally increases.

As an example, line 2 of Table IX relates the flux ratios obtained with hyperosmotic mannitol and sucrose as the tracer solute. The smallest flux asymmetry for this solute pair is seen with the UM-3 membrane which has the largest effective pore radius. The B20 membrane, having a smaller effective pore radius, shows greater flux asymmetry with a flux ratio of 1.57 and the smallest pore membrane, the General Atomic "Type B", shows an even larger flux ratio of 2.89. This progressive increase in flux asymmetry agrees with the hypothesis that the magnitude of the coupling between solute flows and the resulting flux asymmetry is inversely related to the pore radius of the membrane. Indeed such an observation would be expected if coupling between solute flows takes place within the membrane pores since smaller pores require the diffusing solutes to share smaller diffusional spaces, thereby increasing the likelihood of solute interaction.

The effectiveness of a hyperosmotic solute at creating asymmetric solute flow, as measured by the P_{12}/P_{22} term also increases with smaller effective pore radii. This observation is easily demonstrable from the data presented in Table X in which P_{12}/P_{22} values are presented. With only a few exceptions, as the size of the pore decreases, a concomitant increase is seen in the P_{12}/P_{22} values. Again this data agrees with that expected if the pores of the membrane influence the coupling between solute fluxes.

Table X

Comparison of P_{12}/P_{22} Values for Membranes with Differing Effective Pore Radii

Tracer	Solutes Hyperosmotic	$P_{12}/P_{22} \times 10^4$ UM-3*	S&S B20+	G.A. "B"**
Mannitol	M	1.0	6.8	14.9
	S	-	9.2	16.5
	R	4.9	10.1	12.0
Sucrose	M	4.3	9.4	7.0
	S	4.0	10.3	20.3
	R	3.7	12.5	17.8
Raffinose	M	4.9	6.6	5.5
	S	4.7	8.3	18.6
	R	9.3	12.5	19.6

* Approximate effective pore radius = 350 Å
\+ Approximate effective pore radius = 75 Å
** Approximate effective pore radius = 25 Å

M = Mannitol
S = Sucrose
R = Raffinose

This may be visualized by considering that if pores are relatively large, solutes may diffuse through the membrane pores without interacting. However, as the pores of the membrane become smaller, the solutes must use a smaller common diffusional space. Consequently the diffusing hyperosmotic solute acts more effectively to sweep out the solutes within the pore.

In this thesis the major premise advanced is that the physical interaction of solutes in the presence of a concentration gradient is sufficient to account for flux asymmetry. It has been suggested by critics of this explanation that other mechanisms should be considered. One of the suggestions offered was that of the participation of convective water flow. Hence, experiments were carried out to determine whether this convective flow of H_2O could, in some way, be responsible for creating the asymmetric solute flux. In these experiments tritiated water fluxes were determined with hyperosmotic solution bathing one side of the membrane, water bathing the other, and osmotic flow blocked by hydrostatic pressure. Labeled water fluxes were also determined with the hyperosmotic solution bathing both sides of the membrane. If convective flow of water existed across the membrane under experimental conditions, one would expect the HTO fluxes to be larger than the fluxes carried out with hyperosmotic solution bathing both sides of the membrane where the flow of HTO is by diffusion alone. In no case was the tritiated water flow under the experimental conditions larger than under the control conditions. In both cases the

flows of tritiated water were symmetrical, that is no HTO flux asymmetry was observed. These findings suggest that there is no significant convective flow across the membrane and reinforces the fact that no net volume flow of water is taking place under experimental conditions.

DISCUSSION

The discovery of a net flux of a solute across a non-biological membrane, down the concentration gradient of a second diffusible solute, is in accord with the findings on biological membranes reported by Franz and Van Bruggen (7, 76), Ussing (6) and confirmed by Biber and Curran (55). In the relatively wide pore nonbiological membranes used in the experiments reported here, the osmotic flow of water into the hyperosmotic solution had to be countered by the imposition of a hydrostatic pressure on this solution. This requirement is to be expected in wide pore membranes but should not be necessary in the "narrow pore" biological membranes where the $1 - \sigma$ term which is responsible for solvent drag is small.

As a consequence of the initial experiments carried out on the UM-3 membrane one may conclude that it is indeed possible for nonelectrolyte flux asymmetry to be created under conditions analogous to those used in the biological systems. Furthermore, there appears to be no need to invoke the intervention of any biological processes such as the active transport pump initially implicated by Ussing (6).

Since the process has not only magnitude but also is directional, it is clearly a vector quantity. Recalling Curie's theorem (80) that a vectorial flux must be driven by a vectorial

force, one must conclude that the force creating flux asymmetry is vectorial. The only source of force clearly available to the non-biological system is that created by the unequal distribution of the hyperosmotic solute across the membrane.

Osmotic flow of water is an unlikely candidate for the force behind the flux asymmetry since the solvent drag which could create flux asymmetry would tend to increase the flux of solute into the hyperosmotic solution rather than out of it as is observed. Furthermore, it is particularly hard to visualize how an osmotically induced solvent flow could create flux asymmetry when the net volume flow is held at zero as it is in the nonbiological membrane system.

As predicted by equation 9 and confirmed experimentally by Durbin (72) osmotic and hydrostatic flow may be equated. That is, equal amounts of pressure, whether they be osmotic or hydrostatic, will produce equal flows. Consequently, it should be possible to use hydrostatic pressure to block the osmotic flow of solvent across a membrane without fear that a pressure gradient will be created.

Clearly the only remaining vectorial force which could create the observed net flux of solute is the diffusion of the hyperosmotic agent down its concentration gradient. This force, unlike that of osmosis, would be of the proper vectorial sign to produce a net flux of solute out of the hyperosmotic solution. Let us now consider how this diffusion might act to produce asymmetric solute fluxes.

When one looks through a microscope and observes the continuous erratic motion of small suspended particles he is observing a visible manifestation of the mechanism of diffusion (79). This process called Brownian movement is caused by the continuous bombardment of the suspended particles by the molecules in the medium in which they are suspended. A similar sight would probably be seen if a person were able to observe sucrose molecules in a homogeneous 0.35 M solution of sucrose through a "super microscope". Each sucrose molecule would be seen to move randomly about in the solution colliding with water and other sucrose molecules, then moving off in a new direction to a different part of the solution, all at the average speed of about 200 miles per hour (79). Although these molecules move about from one place in the solution to another, the concentration of the solute at any point in the solution never changes significantly since other sucrose molecules move into the volume vacated by the previous ones. Jacobs (79) has calculated, using probability theory, that one could expect a variation of only 0.000,000,012% in the concentration of the solute in a milliliter of 0.5 M sucrose at room temperature, a value clearly undetectable by the best methods of chemical analysis. Hence, in a homogeneous solution there is no net movement of solute to create a concentration gradient. If we were to mix into such a sucrose solution some inulin molecules, we would see under our hypothetical "moleculescope" that the inulin molecules undergo the same Brownian movement as do the

sucrose molecules and visible particles. Although there may be interaction between the sucrose and inulin molecules, no vectorial transfer of inulin will be observed, as the movement of the molecules is completely random.

Now consider a more complicated example of the diffusion process. If we carefully layer a solution of 0.35 M solute such as sucrose under a volume of pure water, an interface can be formed between the two solutions. At this beginning time, the water solution will contain essentially no sucrose. After a period of time, if we again look at the solutions, we will find that the sucrose has spread throughout the total volume and is of the same unit concentration at any point in the solution. In this instance there has been a net flux of the solute from the more concentrated 0.35 M sucrose solution to the pure water. If we observed the process under our hypothetical microscope, we would see the same random collisions taking place between solute and solvent molecules. However, as we watched, we would see that a net movement of solute took place. Molecules moving at velocities roughly equivalent to the speed of a rifle bullet would shoot across the solution just as they did in the homogeneous solution, but the molecules moving into the water from the sucrose solution would not be replaced by sucrose molecules moving from the water, simply because there were none in the pure water compartment of the system. Since diffusion is based on probability (79), as more sucrose molecules move into the water part of

the system, the probability that molecules will diffuse back into the sucrose solution increases. Eventually the sucrose would be spread evenly throughout the system and the solution would be homogeneous. Although the sucrose molecules would continue to diffuse from one half of the system to the other, further net transport of sucrose would not occur.

If both the sucrose and water phases were to be made 1 mM in respect to inulin, an interesting phenomenon would occur when the solutions were brought together. As before, the sucrose would leave the sucrose-inulin phase and diffuse into the water-inulin phase. Inulin, of course, could exchange between the two phases but no net inulin loss or enrichment of either phase is to be expected. However, a net inulin movement will be seen to occur in the direction of the sucrose gradient, that is, the former water-inulin solution will become enriched with inulin, as well as gaining sucrose. This net inulin flux results from the interaction of the sucrose "flow" with the inulin. Since the sucrose is moving under the vectorial force of its concentration gradient its interaction with the inulin molecules imparts a vectorial force to the inulin. As long as there is a movement of sucrose down its concentration gradient, there will be a net flux of inulin in the same direction. This process has been studied for at least 10 solute pairs, including sucrose-mannitol and raffinose-urea. In such free solution systems Albright (81), Ellerton (82), Dunlop (83) and others (84, 85) have shown interaction of flows

to play a significant role in the isothermal diffusion of ternary systems of both electrolytes and nonelectrolytes.

Diffusion in biological transport systems is further complicated by the presence of membranes. Membranes somewhat modify the rate of diffusion by limiting the area at the interface between two solutions and by presenting relatively narrow and sometimes tortuous paths through which the diffusing solute must move.

For a simplified theoretical membrane system, let us consider the diffusion of solutes through a membrane with right cylindrical water-filled pores, all with a pore radius of 10 Å. If we place on one side of the membrane a 0.35 M solution of sucrose ($\sigma > 0$) and on the other a solution of pure water, two processes will take place. Water will move into the sucrose solution by osmosis and simultaneously sucrose will diffuse into the water solution. If this osmotic flow of water into the sucrose solution is blocked, the process of diffusion can be studied without the complicating effect of osmosis. Having eliminated osmotic water flow, sucrose molecules will diffuse to the membrane and proceed to find their way through the water-filled pore, colliding with the walls of the pore, with water, and with other solute molecules. As the size of the test solute increases or the radius of the pore decreases, there will be more interaction of the solute with the walls of the pore, tending to decrease the solute permeability.

Now, if both bathing solutions are made 1 mM with inulin, we will observe a result similar to that observed in the free solution studies, that is, there will be a net flux of inulin into the water even though a concentration gradient for it does not exist.

The process may be visualized in the following way. As a result of random thermal diffusion an inulin molecule finds itself in a pore of the membrane. Here it may move back out of the pore or it may move on through the pore, depending upon which side it is bombarded by molecules in the medium. Inasmuch as all the pores in the membrane are the same size, the inulin will share the pore with the diffusing sucrose molecules. Since the sucrose is diffusing down its concentration gradient, it will collide with the inulin molecule, acting to push it into the inulin-water solution. If this inulin molecule has come from the sucrose-inulin-water solution, the effect of the interaction between the sucrose and the inulin will be to increase the flux of inulin across the membrane. However, if the inulin molecule has diffused into the pore from the inulin-water solution, its interaction with the diffusing sucrose molecules will be to decrease the inulin flux into the sucrose-inulin-water solution. As a result, there will be a net flux of inulin into the inulin-water solution. Such a mechanism is well supported by the observations summarized in Fig. 7 where the increase in outflux is approximately equal to the decrease in the influx of a tracer

solute with an increase in hyperosmotic agent concentrations.

Solutes smaller than inulin would be affected in an identical way but would present a smaller cross-sectional area for collision with the diffusing sucrose so that less interaction would take place between the two species and less asymmetry of flux would be observed. This concept of solute movement agrees well with observations reported in this thesis where increasing tracer size is paralleled by increasing flux asymmetry with any particular diffusing hyperosmotic agent.

As the size of the hyperosmotic agent increases with respect to the size of the pore the rate of diffusion across the membrane would be decreased due both to the greater degree of frictional interaction with the walls of the pore and the decrease in diffusion caused by the increase in molecular mass. However, when a molecule of a larger diffusing hyperosmotic solute gets into the pore, its effectiveness at pushing other solutes out of the pore will be increased. In other words, the increased cross-sectional area and mass of a large hyperosmotic agent will make interactions with other solute molecules more effective once the solute enters a pore. Indeed the effectiveness of a solute as a "driver", measured by P_{12}/P_{22}, generally increases with increasing size of a solute for a given membrane in the experiments reported in this thesis. Furthermore, the effectiveness of any one hyperosmotic agent, again measured

by P_{12}/P_{22}, increases with an increase in the ratio of its size to the effective size of the pores of the membrane. In other words, as the size of the solute approaches the size of membrane pores, its effectiveness of interaction also increases.

When the hyperosmotic agent becomes larger than the pores of the membrane, one would expect the hyperosmotic agent to fail to produce flux asymmetry. Although such experiments were not possible with the membranes used in the present studies due to the limited solubility of solutes larger than the pores of the membrane, Franz and Van Bruggen (7) and Biber and Curran (55) have reported that raffinose, which is relatively impermeable to frog and toad skin, fails to produce flux asymmetry in such systems.

If the model just presented is valid, how do we explain the anomalous behavior seen with the dextrans as the tracer species?

Although the molecular shapes of the dextran preparations used in these experiments are not agreed upon (86, 87), Ingleman and Halling (86) have presented evidence that such preparations are rod shaped rather than spherical when in solution. According to their calculations, the larger dextran (60,000 to 90,000 MW) is some three times the length of the 16,000 to 19,000 MW fraction. The cross-sectional area of the larger species will, however, be only a little larger than that of the smaller species of dextran (see Table II).

Soll (88) has recently presented evidence that, for many solutes, the diffusion coefficient of a solute is proportional to the

length of the molecular specie, whereas the permeability of a solute in the presence of a bulk flow of water is a function of the molecular diameter of the molecule. He suggests that the flow of the water through pores mediates an orientation of the solute with the longitudinal axis of the solute perpendicular to the membrane surface. It may be that the flow of diffusing hyperosmotic agent orients the large dextran in a way similar to that of a bulk flow of water. Hence the permeability of the large dextran fraction increases. The smaller dextran could also be oriented in such a way but may have a greater tendency to tumble in the flow since its length to diameter ratio is smaller than that of the larger species. As a consequence, one might expect the larger of the two dextrans to show a larger increase in permeability than the smaller in the presence of a flow of hypertonic solute across the membrane. It would also be expected that the larger the flow of solute or solvent, the greater would be the orienting effect of the flow on the dextran molecules. Consequently, a larger increase in permeability could be created by the causdtive flow whether it be solvent or solute. If this is true, the larger the osmotic agent, and consequently the smaller the solute flow, the smaller would be the orienting effect of the flow. Hence the difference in permeability between the two dextran fractions should be decreased with the larger hyperosmotic solutes such as raffinose and dextran. Indeed, with raffinose as the osmotic agent, the experimental permeability coefficients of the two dextrans are almost equal. With dextran, a quite

impermeable hyperosmotic agent, the smaller dextran again becomes more permeable than the larger specie as is the case in pure diffusion seen in Figs. 8 and 9. However, in this case it appears that the limited amount of diffusion is unable to affect the relative permeabilities of the two tracer dextrans.

As can be seen in Figs. 12 through 15, the flux ratios obtained with the two dextran tracers do not follow the trend of increasing flux ratios with increasing tracer size established by tracer mannitol through inulin. If the dextrans are rod shaped as suggested by Ingleman and Halling, the effective area for interaction may not be directly proportional to the molecular weight of the tracer molecule due to orienting effects of a solute flow. Consequently, the degree of flux asymmetry may not be proportional to the molecular weight of the molecule. If the orienting effect is present, it would probably be most effective when the flow of osmotic solute is greatest. Assuming this and assuming that the interaction between flows is frictional in nature one may expect the smaller dextran, which has a diameter as well as length smaller than the large dextran, to interact less with the diffusing osmotic agent, creating less flux asymmetry. As the permeability of the osmotic agent decreases it might be expected that the smaller dextran would be oriented less stably and collisional interactions with the diffusing solute would become more effective in producing large flux ratios. As can be seen in Figs. 11, 12 and 13 and Table XI, the flux ratio of the smaller dextran

Table XI

P^{*} Values and Flux Ratios of Dextrans I and II on S&S B20 Membrane

	Dextran I (16,000-19,000 MW)	Dextran II (60,000-90,000 MW)
H_2O Both ± 1 SE	10.0 ± 0.3	9.8 ± 0.2
Hyperosmotic agent		
1. Mannitol		
Outflux ± 1 SE	11.0 ± 0.4	15.2 ± 0.6
Influx ± 1 SE	8.5 ± 0.4	8.1 ± 0.4
Flux Ratio	1.3	1.9
2. Sucrose		
Outflux ± 1 SE	13.9 ± 0.2	22.2 ± 0.9
Influx ± 1 SE	4.7 ± 0.4	6.4 ± 0.2
Flux Ratio	3.0	3.5
3. Raffinose		
Outflux ± 1 SE	18.5 ± 1.3	18.2 ± 0.2
Influx ± 1 SE	5.0 ± 0.6	7.0 ± 0.4
Flux Ratio	3.7	2.6
4. Dextran^{+}		
Outflux ± 1 SE	34.5 ± 1.2	13.9 ± 0.3
Influx ± 1 SE	23.7 ± 1.1	9.4 ± 0.7

$^{*}P = x10^{3}$ (cm hr^{-1})

$^{+}\sim 0.008$ m

is much less than that for the larger dextran tracer when the extremely permeable mannitol is the hyperosmotic solute. The flux ratio of this smaller dextran is increased with the less permeable sucrose osmotic agent and is actually larger than the flux ratio for the large dextran when the less permeable raffinose is the driver solute.

To this point in the discussion, membranes have been assumed to be homoporous, consisting entirely of right cylindrical pores of equal size and uniform length. In reality, it is naive to think of biological membranes or even the synthetic membranes studied here as being of such a simplified construction.

The "pore", as it exists in the membrane, is probably far from being a right cylinder or even a tube at all. Indeed, the membrane matrix is probably more correctly visualized as a maze of interconnecting channels. These channels, or open spaces between the ultrastructural components of the membrane, form continuous tortuous pathways across the membrane through which solutes may diffuse. In membrane matrices such as these, the selectivity of the membrane to the diffusion of solutes is determined by the size of the spaces between the solid structural constituents of the membrane. Small solutes may diffuse through any of the interspaces within the membrane matrix while larger solutes must use pathways made up of spaces which are large enough to accept these larger molecules. As a consequence, the permeability of larger solutes will be lower since

the number of "pores" through which they may diffuse is smaller and the pathway through which diffusion may take place is more tortuous. This concept of structure has a direct bearing upon solute interaction, for it may be that such an increase in the pore length increases the amount of potential interaction between solute flows by increasing the length of time that the hyperosmotic and tracer solutes are entrained within the membrane matrix.

The concept that a maze of open spaces between membrane constituents makes up the pores suggests that the pores so created will not be of uniform size and that there will thus exist a spectrum of pore sizes of which the effective pore radius is only an approximation of the average value. Some of the pores will be larger than the ideal effective pore and as is suggested by the model presented here, the magnitude of interaction in these pores will be smaller than the interaction in pores with the radius of the effective pore. Conversely, there will also be pores smaller than the effective pore. In some of these smaller pores the coupling of solute flows will be large while in others, no interaction between the solutes will take place due to the fact that one or both of the solutes are excluded from the membrane. Consequently, it is easy to see that the pore size distribution is of paramount importance in determining the magnitude of the flux asymmetry which may be observed in a membrane. These reasons alone are enough to cause one to expect significant variability in the magnitude of the flux asymmetry from one membrane

type to another, although both may have the same effective pore radius.

The demonstration that coupling of solute flows can take place in synthetic as well as biological membranes shows that the phenomenon is physical in nature and must be considered as a potential creator of solute flux in all membranes.

Hence the equation,

$$J_i = C_i (1 - \sigma) J_v + P_{ii}\Delta C_i \qquad (19)$$

developed by Kedem and Katchalsky (48) to describe the passive flux of solute across a membrane does not adequately describe a system with two or more permeable solutes. For each solute, j, which may couple flows with solute i, a solute drag term must be added to the equation above, which as it stands includes only the contributions of solvent drag and self diffusion. The "cross term" expression which may be used to describe solute drag is $P_{ij}\Delta C_j$. P_{ij} is the cross term permeability coefficient describing the permeability of solute i caused by solute j, and ΔC_j is the concentration gradient of solute j.

The equation which results may be written as,

$$J_i = C_i (1 - \sigma) J_v + P_{ii}\Delta C_i + \sum_{\substack{j=o \\ j\neq i}}^{n} P_{ij} C_j \qquad (39)$$

where $\sum_{\substack{j=o \\ j\neq i}}^{n} P_{ij}\Delta C_j$ quantitates the total effect of the coupling of

solute flows on the net flux of solute i.

The above equation suggests that for any membrane, whether it be biological or nonbiological, the possibility of coupling between solute flows exists as a possible means of creating net solute flux if there are two or more solute species in the bathing solutions. It may be that solute i will have a concentration gradient opposite to that of solute j. If there is interaction between the two flows the effect of solute j will be to decrease the flux of solute i. On the other hand, if solute i has no concentration gradient or if the concentration gradient is in the same direction as solute j, the effect of the solute interaction will be to increase the net flux of solute i. As can be seen in equation 39, if either P_{ij} or ΔC_j is equal to zero, there will be no solute drag effect of solute j on solute i.[3]

Solute drag may be important in explaining some of the problems faced in the field of membrane transport. One of these problems is the matter brought up by Ling (89) in which there is concern that calculations of the amount of ATP required to drive all active transport pumps, postulated to exist in the cell, far exceed the ATP available. In other words it is suggested that the cell cannot possibly supply enough metabolic energy to do the work of actively transporting all the solutes proposed to be actively transported across the cell membrane. A resolution of this dilema offered by

[3]There is no experimental evidence that P_{12} may be negative in the systems which have been studied.

this thesis is to postulate a coupling of flows between one actively transported solute such as sodium ions and a second solute such as a sugar or amino acid. In this way both solutes could be transported at the expense of a single metabolically driven pump.

Alternatively, a coupling of solute fluxes could take place between a solute for which a concentration gradient exists and the second solute not having a chemical potential to diffuse. Such an instance might be the coupling of a sugar with sodium ions which have a gradient in which the extracellular Na^+ concentration is much higher than on the inside of the cell. As the Na^+ diffuses into the cell it might drag with it the sugar creating a net influx of the carbohydrate. Hence, no matter what biological membrane system one is concerned with, solute drag must be considered as a potentially important transport process.

CONCLUSION

Experiments presented in this thesis have shown that it is possible to create, in completely nonbiological membranes, hyperosmotically inducible asymmetric solute flows analogous to those observed with biological systems. Evidence has been presented that this flux asymmetry is created by the interaction between the diffusional flows of the hyperosmotic agent, having a concentration gradient, and the tracer solute having no concentration gradient. This net flux is shown to be caused both by the increase of tracer solute flux down the concentration gradient of the hyperosmotic solute and a decrease in the flux of tracer solute into the hyperosmotic solution. Experiments carried out with solutes of varying size as well as with membranes varying in their effective pore radii show that the phenomenon being investigated is directly proportional to the sizes of the solute species and inversely proportional to the pore radius of the membrane.

A model has been proposed to explain the mechanism of solute drag on the basis of frictional interaction between solute species.

ACKNOWLEDGEMENTS

I wish to thank Dr. J. T. Van Bruggen whose encouragement and guidance have made the time spent in his laboratory a valuable learning experience. His advice and direction have greatly aided the work presented in this thesis. Special thanks is extended to Mrs. Jean C. Scott and Mr. Barry M. Trowbridge for their excellent technical assistance, and to Mrs. Mary Buck for the preparation of this manuscript.

This work was supported largely by research contract AT(45-1)-1754 from the United States Atomic Energy Commission. Financial support through a National Institutes of Health predoctoral fellowship, 5 T01 GM1200, is gratefully acknowledged. Supplementary support was provided by grant AM 07201 from the United States Public Health Service.

REFERENCES

1. Barnes, T. C. The influence of heavy water and temperature on the electrical potential of frog skin. J. Cell. and Comp. Physiol., 1939. 13, 39-50.

2. Lindley, B. D., Hoshiko, T., & Leb, D. E. Effects of D_2O and osmotic gradients on potential and resistance of the isolated frog skin. J. Gen. Physiol., 1964. 47, 773-793.

3. Ussing, H. H., & Andersen, B. The relation between solvent drag and active transport of ions. Proc. IIIrd Int. Congr. Biochem. Brussels. New York, N.Y.: Academic Press, 1955. 434-440.

4. Ussing, H. H., & Windhager, E. E. Nature of shunt pathway and active transport path through frog skin epithelium. Acta Physiol. Scand., 1964. 61, 484-504.

5. Ussing, H. H. Relationship between osmotic reactions and active sodium transport in the frog skin epithelium. Acta Physiol. Scand., 1965. 63, 141-155.

6. Ussing, H. H. Anomolous transport of electrolytes and sucrose through the isolated frog skin induced by hypertonicity of the outside bathing solution. Ann. N.Y. Acad. Sci., 1966. 137, 543-555.

7. Franz, T. J., & Van Bruggen, J. T. A possible mechanism of action of DMSO. Ann. N.Y. Acad. Sci., 1967. 141, 302-309.

8. Franz, T. J., Galey, W. R., & Van Bruggen, J. T. Further observations on asymmetrical solute movement across membranes. J. Gen. Physiol., 1968. 51, 1-12.

9. Biber, T. U. L., & Curran, P. F. Coupled solute fluxes in frog skin. Biophys. J., 1968. 8, A127.

10. Stein, W. D. The Movement of Molecules Across Cell Membranes. New York: Academic Press, 1967. p. 207.

11. Landis, E. M., & Pappenheimer, J. R. In P. Dow and W. F. Hamilton (Eds.) Handbook of Physiology Section 2: Circulation. Vol. 2. Washington, D. C.: American Physiological Society, 1963. 29.

12. Brown, A. C., & Masoro, E. J. Absorption from the gastrointestinal tract. In T. C. Ruch & H. D. Patton (Eds.) Physiology and Biophysics. Philadelphia, Pa.: W. B. Saunders Co., 1966. pp. 997-1007.

13. Keynes, R. D. The ionic movements during nervous activity. J. Physiol., 1951. 114, 119-150.

14. Woodbury, D. M. Physiology of body fluids. In T. C. Ruch & H. D. Patton (Eds.) Physiology and Biophysics. Philadelphia, Pa.: W. B. Saunders Co., 1966. p. 893.

15. Koch, A. The kidney. In T. C. Ruch & H. D. Patton (Eds.) Physiology and Biophysics. Philadelphia, Pa.: W. B. Saunders Co., 1966. pp. 843-870.

16. Renkin, E. M. Capillary permeability to lipid-soluble molecules. Am. J. Physiol., 1952. 168, 538-545.

17. Holter, H. Pinocytosis. In G. W. Wolstenholme (Ed.) Ciba Found. Symp.: Enzyme and drug action. Boston, Mass.: Little, Brown and Co., 1962.

18. Palade, G. E. Transport in quanta across the endothelium of blood capillaries. Anat. Rec., 1960. 136, 254.

19. Goldstein, D. A., & Solomon, A. K. Determination of equivalent pore radius for human red cells by osmotic pressure measurement. J. Gen. Physiol., 1960. 44, 1-17.

20. Koefoed-Johnsen, V., & Ussing, H. H. The contributions of diffusion and flow to the passage of D_2O through living membranes. Effect of neurohypophyseal hormone on isolated anuran skin. Acta Physiol. Scand., 1953. 28, 60-76.

21. Ross, E. J. The transfer of non-electrolytes across the blood-aqueous barrier. J. Physiol., 1951. 112, 229-237.

22. Le Fevre, P. G. Evidence of active transfer of certain non-electrolytes across the human red cell membrane. J. Gen. Physiol., 1948. 31, 505-527.

23. Widdas, W. T. Inability of diffusion to account for placental glucose transfer in sheep and consideration of the kinetics of a possible carrier transfer. J. Physiol. (London), 1952. 118, 23-39.

24. Rosenburg, F., & Wilbrandt, W. Uphill transport induced by counter-flow. J. Gen. Physiol., 1957. 41, 289-296.

25. Dainty, J., & Ginzburg, B. Z. The reflection coefficient of plant cell membranes for certain solutes. Biochim. Biophys. Acta, 1964. 79, 102-129.

26. Pappenheimer, J. R., Renkin, E. M., & Borreo, L. M. Filtration, diffusion and molecular sieving through peripheral capillary membranes. A contribution to the pore theory of capillary permeability. Am. J. Physiol., 1951. 167, 13-46.

27. Paganelli, C. V., & Solomon, A. K. The rate of exchange of tritiated water across the human red cell membrane. J. Gen. Physiol., 1957. 41, 259-277.

28. Fick, A. Ueber diffusion. Paggend. Ann., 1855. 94, 59-86.

29. Andersen, B., & Ussing, H. H. Solvent drag on non-electrolytes during osmotic flow through isolated toad skin and its response to antidiuretic hormone. Acta Physiol. Scand., 1957. 39, 229-239.

30. Ginzburg, B. Z., & Katchalsky, A. Frictional coefficients of the flows of non-electrolytes through artificial membranes. J. Gen. Physiol., 1963. 47, 403-418.

31. Skou, J. C. Enzymatic basis for active transport of Na^+ and K^+ across cell membrane. Physiol. Review, 1965. 45, 596-617.

32. Post, R. L., Sen, A. K., & Rosenthal, A. S. A phosphorylated intermediate in adenosine triphosphate-dependent sodium and potassium transport across kidney membranes. J. Biol. Chem., 1965. 240, 1437-1445.

33. Bader, H., Sen, A. K., & Post, R. G. Isolation and characterization of a phosphorylated intermediate in the (Na^+ + K^+) system-dependent ATPase. Biochim. Biophys. Acta, 1966. 118, 106-115.

34. Hoffman, J. F. The cellular functions of membrane transport. Englewood Cliffs, New Jersey: Prentice Hall, 1964.

35. Overbeek, J. Th. G. The Donnan equilibrium. Prog. Biophys. Biophys. Chem., 1956. 6, 57-84.

36. Einstein, A. Investigations on the theory of the Brownian movement. 1905 (English translation and notes by R. Farth) Reprint: Dover, New York, 1956.

37. Einstein, A. On the movement of small particles suspended in a stationary liquid demanded by the molecular-kinetic theory of heat. Ann. Physik., 1905. 17, 549.

38. Einstein, A. On the theory of the Brownian movement. Ann. Physik., 1906. 19, 371-381.

39. Dick, D. A. T. Cell water. Washington, D. C.: Butterworth, Inc., 1965. pp. 15-43.

40. Glasstone, S. Textbook of physical chemistry, Second Edition. New York: D. Van Nostrand, 1946. pp. 663-668.

41. van't Hoff, J. H. Die Rolle des osmotichen Druches in der analogie zwichen Lösungen und Gasen. Physikal. Chem., 1887. 1, 481-508.

42. Staverman, A. J. Non-equilibrium thermodynamics of membrane processes. Trans. Faraday Soc., 1952. 48, 176-185.

43. De Groot, S. R. Thermodynamics of irreversible processes. Amsterdam: North Holland Publishing Co., 1963.

44. Stein, W. D. The movement of molecules across cell membranes. New York: Academic Press, 1967. p. 41.

45. Onsager, L. Reciprocal relations in irreversible processes. Phys. Rev., 1931. 37, 405.

46. Pirigogine, I. Introduction to thermodynamics of irreversible processes. New York: J. Wiley and Sons, 1962.

47. Van Ryssolberghe, . Thermodynamics of irreversible processes. New York: Blaisde Publishing Co., 1963.

48. Kedem, O., & Katchalsky, A. Thermodynamic analysis of the permeability of biological membranes to non-electrolytes. Biochim. Biophys. Acta, 1958. 27, 229-246.

49. Kedem, O., & Katchalsky, A. A physical interpretation of the phenomenological coefficients of membrane permeability. J. Gen. Physiol., 1961. 45, 143-179.

50. Curran, P. F., & Katchalsky, A. Nonequilibrium thermodynamics in biophysics. Cambridge, Mass.: Harvard University Press, 1965.

51. Kirkwood, J. G. Transport of ions through biological membranes from the standpoint of irreversible thermodynamics. In H. T. Clarke (Ed.) Ion transport across membranes. New York: Academic Press, 1954. pp. 119-127.

52. Coster, H. G. L., & George, E. P. A thermodynamic analysis of fluxes and flux ratios in biological membranes. Biophys. J., 1968. 8, 457-469.

53. Staverman, A. J. Theory of measurement of osmotic pressure. Rec. Trav. Chim., 1951. 70, 344-352.

54. Stein, W. D. The movement of molecules across biological membranes. New York: Academic Press, 1967. p. 41-48.

55. Biber, T. U. L., & Curran, P. F. Coupled solute fluxes in frog skin. J. Gen. Physiol., 1968. 51, 606-620.

56. Woolf, L. A., Miller, D. G., & Gosting, L. J. Isothermal diffusion measurements on the system H_2O-glycine-KCl at 25°; tests of the Onsager reciprocal relation. J. Am. Chem. Soc., 1962. 84, 317-327.

57. Markley, L. L., Bixler, H. J., & Cross, R. A. Utilization of polyelectrolyte complexes in biology and medicine. J. Biomed. Mater. Res., 1968. 2, 145-155.

58. Schleicher & Schuell Co., S & S membrane filters and apparatus Bulletin #79. Keene, New Hampshire. March, 1963.

59. Riley, R., Gardner, J. O., & Merten, U. Cellulose acetate membranes: electron microscopy of structure. Science, 1964. 143, 801-803.

60. Stecher, P. G. (Ed.) The Merck index of chemicals and drugs, Seventh Edition. Rahway, New Jersey: Merck and Company Inc., 1960. 637, 896.

61. Tanford, C. Physical chemistry of macromolecules. New York: John Wiley and Sons, 1961. pp. 210-212.

62. Buhler, D. R. A simple scintillation counting technique for assaying $C^{14}O_2$ in a Warburg flask. Anal. Biochem., 1962. 4, 413-417.

63. Van Bruggen, J. T., & Scott, J. C. Microdetermination of carbon dioxide. Anal. Biochem., 1962. 3, 464-471.

64. Wilzbach, K. E. Tritium-labeling by exposure of organic compounds to tritium gas. J. Am. Chem. Soc., 1957. 79, 1013.

65. Wilzbach, K. E. The gas exposure technique for tritium labeling. In S. Rothchild (Ed.) Advances in tracer methodology. Volume 1. New York, N. Y.: Plenum Press, 1962. pp. 4-11.

66. Frush, H. L. Large-scale, preparative paper chromatography. J. Res. Nat. Bur. Stand., 1967. 71A, 49-52.

82. Ellerton, H. D., & Dunlop, P. J. Diffusion and frictional coefficients for four compositions of the system water-sucrose-mannitol at 25°. Tests of the Onsager reciprocal relation. J. Phys. Chem., 1967. 71, 1291-1297.

83. Dunlop, P. J. Interacting flows in diffusion of the system raffinose-urea-water. J. Phys. Chem., 1957. 61, 1619-1622.

84. Fujita, H., & Gosting, L. J. An exact solution of the equations for free diffusion in three-component systems with interacting flows and its use in evaluation of diffusion coefficients. J. Am. Chem. Soc., 1956. 78, 1099-1106.

85. Baldwin, R. L., Dunlop, P. J., & Gosting, L. J. Interacting flows in liquid diffusion: Equations for the evaluation of the diffusion coefficients from movements of the refractive index gradient curves. J. Am. Chem. Soc., 1955. 77, 5235-5249.

86. Ingleman, T., & Halling, M. S. Some physicochemical experiments on fractions of dextran. Arkiv. Kemi., 1949. 1, 61-80.

87. Ogston, A. G., & Woods, E. F. Molecular configuration of dextrans in aqueous solution. Nature, 1953. 171, 221-222.

88. Soll, A. A new approach to molecular configuration applied to aqueous pore transport. J. Gen. Physiol., 1967. 50, 2565-2578.

89. Ling, G. N. The membrane theory and other views for solute permeability, distribution, and transport in living cells. Perspectives Biol. Med., 1965. 9, 87-106.

90. Ling, G. N. A physical theory of the living state. Boston: Ginn, 1962.

67. Frush, H. L. Personal Communication. 1968.

68. Franz, T. J. The effect of hyperosmotic agents on frog skin. Unpublished masters dissertation, Univ. of Oregon Med. School, 1965. p. 46-47.

69. Moir, N. J. The metabolism of ethanol. Unpublished masters dissertation, Univ. of Oregon Med. School, 1966. p. 27.

70. Bray, G. A. A simple efficient liquid scintillator for counting aqueous solutions in a liquid scintillation counter. Anal. Biochem., 1960. 45, 279-285.

71. Gordon, C. F., & Wolf, A. L. Liquid scintillation of aqueous samples. Anal. Chem., 1960. 32, 574.

72. Durbin, R. P. Osmotic flow of water across permeable cellulose membranes. J. Gen. Physiol., 1960. 44, 315-326.

73. Renkin, E. M. Filtration, diffusion and molecular sieving through porous cellulose membranes. J. Gen. Physiol., 1954. 38, 225-243.

74. Hays, R. M., & Leaf, A. Studies on the movement of water through the isolated toad bladder and its modification by vasopressin. J. Gen. Physiol., 1962. 45, 933-948.

75. Stein, W. D. The movement of molecules across cell membranes. New York: Academic Press, 1967. p. 111.

76. Franz, T. J., & Van Bruggen, J. T. Hyperosmolarity and the net transport of nonelectrolytes in frog skin. J. Gen. Physiol., 1967. 50, 933-949.

77. Sidel, V. W., & Solomon, A. K. Entrance of water into human red cells under osmotic pressure gradient. J. Gen. Physiol., 1957. 41, 243-257.

78. Barton, T. C., & Brown, D. A. J. Water permeability of the foetal erythrocyte. J. Gen. Physiol., 1964. 47, 839-849.

79. Jacobs, J. H. Diffusion processes. Ergebnisse der Biologie, 1935. 12, 1-160.

80. Curie, P. "Oeuvres" Paris: Gauthier-Villars, 1908. pp. 118-141.

81. Albright, J. G., & Mills, R. A study of diffusion in the ternary system, labeled urea-urea-water, at 25° by measurement of the intra-diffusion coefficients of urea. J. Phys. Chem., 1965. 69, 3120-3126.